

University of Denver

Digital Commons @ DU

Electronic Theses and Dissertations

Graduate Studies

1-1-2009

Image Processing of OCT Glaucoma Images and Information Theory Analysis

Shuting Wang
University of Denver

Follow this and additional works at: <https://digitalcommons.du.edu/etd>



Part of the [Life Sciences Commons](#), [Medical Specialties Commons](#), and the [Optometry Commons](#)

Recommended Citation

Wang, Shuting, "Image Processing of OCT Glaucoma Images and Information Theory Analysis" (2009). *Electronic Theses and Dissertations*. 687.
<https://digitalcommons.du.edu/etd/687>

This Thesis is brought to you for free and open access by the Graduate Studies at Digital Commons @ DU. It has been accepted for inclusion in Electronic Theses and Dissertations by an authorized administrator of Digital Commons @ DU. For more information, please contact jennifer.cox@du.edu, dig-commons@du.edu.

IMAGE PROCESSING OF OCT GLAUCOMA IMAGES AND
INFORMATION THEORY ANALYSIS

A Thesis Presented to
the Faculty of Engineering and Computer Science
University of Denver

In Partial Fulfillment
of the Requirements for the Degree
Master of Science

by

Shuting Wang

August 2009

Advisor: Dr. Roger E Salters

Author: Shuting Wang

Title: IMAGE PROCESSING OF OCT GLAUCOMA IMAGES AND INFORMATION THEORY ANALYSIS

Advisor: Roger E Salters

Degree Date: August 2009

ABSTRACT

Glaucoma is a group of optic nerve disease with progressive structural changes leading to loss of visual function. A careful examination and detection of changes in the optic nerve is the key to early diagnosis of glaucoma. Optical Coherence Tomography (OCT) is one of the known techniques of diagnosis of glaucoma. The patients' eyes are scanned and sub-surface images are captured from optical nerves. Captured OCT images usually suffer from noise and therefore image enhancement techniques can help doctors in better analysis of OCT images and diagnosis of glaucoma. In this thesis, we propose three successful algorithms for enhancing the quality and the contrast of OCT images. Our experiments on sample OCT images show that our algorithms can remove noise and disturbance in images and significantly enhance the visual quality of the glaucoma images. Information theory is widely used in image processing these years. It is proved that information theory is very useful to show the trends between the systems. By using information theory, the ability of each algorithm in enhancing the quality of OCT images is examined. Information theory helped us to find out the relationships of the algorithms. In this research, we use sequential images taken in different time of a same patient and compare the health level of them with the help of Information theory. Information theory successfully helped to provide trends among the sequential images, which will help doctors to diagnosis.

ACKNOWLEDGEMENTS

Great thanks to Dr. Salters, Dr. Mayer, Dr. Fogleman and Dr. Valavanis. During these two years, Dr. Salters teaches me and guides me with patience. I am encouraged and becoming more productive. Dr. Salters is a very knowledgeable professor and I learned more during the two years. Thanks to Dr. Mayer about the research images. Dr. Fogleman and Dr. Valavanis gave me some useful suggestions to this research.

TABLE OF CONTENTS

LIST OF TABLES	vii
LIST OF FIGURES	viii
CHAPTER 1 INTRODUCTION	1
1.1 Introduction	1
1.2 Background	3
1.2.1 Glaucoma and Glaucoma Images	3
1.2.2 Overview of Optical Coherence Tomography (OCT)	4
1.2.3 OCT Images	6
1.3 Digital Image Processing and Image Enhancement	6
1.3.1 Digital Image Processing	6
1.3.2 Image Enhancement and Methods	8
1.3.3 Enhancement Algorithms Used in Glaucoma Images	9
1.4 Information Theory in the Analysis of the Images	10
CHAPTER 2 LITERATURE REVIEW	12
2.1 Image Enhancement Algorithms Used in Glaucoma Images	12
2.2 Principle of OCT	14
2.3 Glaucoma	15
2.4 Information Theory	16
2.5 Research Questions	17
CHAPTER 3 ALGORITHMS USED ON GLAUCOMA IMAGES AND THE MATHEMATICAL THEORY	21
3.1 The Enhancement Algorithms	21
3.1.1 Wavelet Algorithm	21
3.1.2 Sobel Algorithm (Sobel Operator and Blurring Filter)	23
3.1.3 Contrast Adjustment Algorithm	25
3.2 Mathematics in the Algorithms, OCT and Information Theory	26
3.2.1 Mathematics in Enhancement Algorithms	27
3.2.1a Wavelet Decomposition in Wavelet Algorithm	27
a Definition of DWT	27
b Matlab Algorithm	28
3.2.1b Sobel Operator in Sobel Algorithm	31
3.2.1c YCbCr Color Space and Contrast Adjustment	33
3.2.2 Mathematics in Information Theory	34
3.2.2a Entropy	35
3.2.2b Relative Entropy	35
3.2.2c Mutual Information	38
3.2.3 Correlation Analysis	40
3.2.3a Definition of Correlation	40

3.2.3b Mathematical Properties	40
3.2.4 Mathematics in Optical Coherence Tomography (OCT)	41
3.2.4a Interferometry Principle	41
3.2.4b Time Domain OCT	44
3.2.4c Frequency Domain OCT (FD-OCT)	46
3.2.4d Image Acquisition and Display	49
3.2.4e Conclusion	51
3.3 Comments on Each Algorithm	52
3.3.1 The Wavelet Algorithm	53
3.3.2 Sobel Algorithm	54
3.3.3 Contrast Adjustment Algorithm	55
CHAPTER 4 RESULTS OF IMAGE PROCESSING AND INFORMATION THEORY ANALYSIS	56
4.1 Original Glaucoma Images Used in this Research	56
4.2 Resulting Images of the Three Algorithms	59
4.3 Information Theory Results	62
4.3.1 Information Theory Data in Patient A	63
4.3.2 Information Theory Data in Patient B	66
4.3.3 Inner Comparison of Sequential Images of Patient A and Patient B	69
4.4 Results of Correlation	72
4.5 Histograms	76
CHAPTER 5 DISCUSSIONS AND FUTURE RESEARCH	81
5.1 Comparative Analysis of Algorithms	81
5.1.1 Results of Wavelet Algorithm	82
5.1.2 Results of Sobel Algorithm	82
5.1.3 Results of Contrast Adjustment Algorithm	83
5.2 Analysis of Information Theory Results	84
5.2.1 Entropy Results	84
5.2.2 Relative Entropy Results	87
5.2.3 Mutual Information Results	90
5.2.4 Gamma	91
5.2.5 Correlation Results	93
5.3 Best Method	94
5.4 Future Work	97
5.4.1 Modifying Wavelet Algorithm	97
5.4.2 Removing Blue from Glaucoma Images	98
5.4.3 Edge Detection	98
5.4.4 Distance Measurement	99
5.5 Conclusion	100
List of References	102
Disclaimer	104

LIST OF TABLES

Table	Page
Table 1 Summarized Information Theory Results for Patient A in 2005	63
Table 2 Summarized Information Theory Results for Patient A in 2007	64
Table 3 Summarized Information Theory Results for Patient A in 2008	65
Table 4 Summarized Information Theory Results for Patient B in 2005	66
Table 5 Summarized Information Theory Results for Patient B in 04/11/2007	67
Table 6 Summarized Information Theory Results for Patient B in 04/17/2007	68
Table 7 Inner Comparison of Sequential Images of Patient A	70
Table 8 Inner Comparison of Sequential Images of Patient B	71
Table 9 Correlation of Patient A Images in Different Periods	72
Table 10 Correlation of Patient B Images in Different Periods	72
Table 11 Correlation of Patient A Images in Different Enhancement Methods	73
Table 12 Correlation of Patient B Images in Different Enhancement Methods	74
Table 13 Different Gamma Values of Patient A in 2005	75

LIST OF FIGURES

Figure	Page
Figure 1.1 Glaucoma image scanned by OCT	4
Figure 1.2 Fundamental steps in digital image processing	8
Figure 2.1 Glaucoma image (Macular) scanned by OCT	18
Figure 2.2 The cross sectional image	18
Figure 3.1 The flow chart for the wavelet algorithm	23
Figure 3.2 Sobel Operators	24
Figure 3.3 The flow chart for the Sobel algorithm	25
Figure 3.4 The flow chart for the Contrast Adjustment algorithm	26
Figure 3.5 2D DWT of Matlab algorithm	29
Figure 3.6 The Haar wavelet	30
Figure 3.7 The averaging filter used in this Sobel algorithm	33
Figure 3.8 Block diagram of an OCT system	43
Figure 3.9 The basic block diagram of TD-OCT	45
Figure 3.10 FD-OCT optical system structures	47
Figure 3.11 The simulation of interferogram under sample test: (a)spectrum interferogram; (b) time function interferogram	48
Figure 3.12 The block diagram of frame grabber	50
Figure 4.1 Glaucoma image of Patient A in 2005	57
Figure 4.2 (a) Glaucoma image of Patient A in 2007 (b) Glaucoma image of patient A in 2008	57

Figure 4.3 (a) Glaucoma image of Patient B in 2005 (b) Glaucoma image of Patient B in 04/11/2007 (a) Glaucoma image of Patient B in 04/18/2007	58
Figure 4.4 (a) (b) (c) (d) Original image, Wavelet result, Sobel result and Contrast adjustment result of Patient A in 2005, respectively	59
Figure 4.5 (a) (b) (c) (d) Original image, Wavelet result, Sobel result and Contrast adjustment result of Patient A in 2007, respectively	60
Figure 4.6 (a) (b) (c) (d) Original image, Wavelet result, Sobel result and Contrast adjustment result of Patient A in 2008, respectively	60
Figure 4.7 (a) (b) (c) (d) Original image, Wavelet result, Sobel result and Contrast adjustment result of Patient B in 2005, respectively	61
Figure 4.8 (a) (b) (c) (d) Original image, Wavelet result, Sobel result and Contrast adjustment result of Patient B in 04/11/2007, respectively	61
Figure 4.9 (a) (b) (c) (d) Original image, Wavelet result, Sobel result and Contrast adjustment result of Patient B in 04/11/2007, respectively	62
Figure 4.10 Histograms of Sequential OCT Images of Patient A	76
Figure 4.11 Histograms of Sequential OCT Images of Patient B	77
Figure 4.12 Histograms of OCT Images of Patient A in 2005	77
Figure 4.13 Histograms of OCT Images of Patient A in 2007	78
Figure 4.14 Histograms of OCT Images of Patient A in 2008	78
Figure 4.15 Histograms of OCT Images of Patient B in 2005	79
Figure 4.16 Histograms of OCT Images of Patient B in 04/11/2007	79
Figure 4.17 Histograms of OCT Images of Patient B in 04/18/2005	80
Figure 5.1 (a) (b) (c) (d) are FFT plots of original image, wavelet image, sobel image and contrast adjustment image of Patient A in 2005, respectively	85
Figure 5.2 Block diagram of the process	98

CHAPTER 1

INTRODUCTION

1.1 Introduction

To present this research, allow me to introduce some concepts of image enhancement, OCT (Optical Coherence Tomography) scanned glaucoma images and information theory, and also allow me to provide some discussions of how these concepts are used in defining and supporting the research.

Image enhancement is a very popular area in digital image processing, which can include the injection of distortion in order to enhance visual effects of images. The specific technology and methodology depend on the different usage of different images. The results of digital image processing should provide information for a specific application than for the original images. Many digital images need to be enhanced because of blur, edge deletion and so on. Here in this research, the Glaucoma images need to be enhanced, through the use of blurring filters.

Doctors (Ophthalmologists) obtain scanned images of the back of the human eyes from OCT image in an effect to diagnose the level of glaucoma, a kind of eye disease. We refer this kind of images as glaucoma images since they have provided good indicates of whether a patient has glaucoma. However, the glaucoma images scanned by the OCT are not very clear because of the presence of unwanted artifacts. Such images can be a valuable source for doctors to diagnosis the level of glaucoma in each patient, but the details of the images are generally not too good.

In this research, the researcher has two main tasks: first one is applying image enhancement on different glaucoma images using different methods in order to show structures clearer than original images and to give more information to doctors so that they may perform a more complete diagnosis of where the patient has glaucoma and to which level.

Some researchers used information theory in image processing for years [14], also it has proven to be very useful in showing the trends in the behavior between the systems. Therefore a further task for the researcher is to use information theory to find the relationships between the image processing algorithms. Toward that, the researcher will use sequential images taken in different time of a same patient and compare the tissue health level between them. Information theory will provide trend information of the sequential images, which can help doctors to diagnosis the state of glaucoma in patients.

We will discuss the details of digital image processing and image enhancement algorithms and how to apply information theory in sections 1.3 and 1.4, respectively, and in Chapter 3.

1.2 Background

In this section, we will introduce the background in this research. First we introduce Glaucoma and Glaucoma Images, second we will introduce the OCT systems and its images. All of the original OCT images are from Medical School of Yale University.

1.2.1 Glaucoma and Glaucoma Images

Glaucoma is a group of diseases of the optic nerve with some structural changes in a characteristic pattern of optic neuropathy. It is an irreversible disease which will lead to blindness. It is considered to be the second cause of blindness nowadays. In US, there are about 2 million people suffer from glaucoma [13].

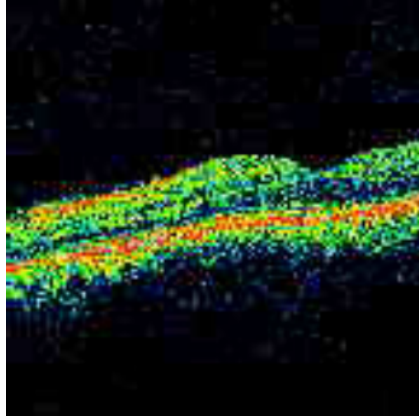


Figure 1.1 Glaucoma image scanned by OCT

The image in Figure 1.1 is scanned by OCT. It represents the layers and cells in the eye. Different colors in the image show different layers and cells in the eye. Doctors (ophthalmologists) would like programs and processes that will highlight different layers where pathologies are. If the layers are really different from each other, in colors or in contrast, then it will be more convenient for doctors to determine which layers are healthy. Such determination is made from the distances between the layers (structures) in the OCT images. Since the contrast of the layers is important for the research, image enhancement methods and algorithms must be applied to the OCT images.

1.2.2 Overview of Optical Coherence Tomography (OCT)

In this research, all images are taken by OCT. Optical techniques are very important in biological medicine. It is safe, cheap and offers a therapeutic potential [9].

Optical coherence tomography (OCT) is a widely used imaging technology for diagnosis which can provide with high-resolution cross-sectional images of different part of tissues [11]. Its first applications in medicine and diagnosis is in less than a decade ago [15], [16].

OCT is widely used in biological medicine simply because it is safe and can generate high-resolution images. At present, OCT is used in three-dimensions (3-D) of optical imaging, in macroscopic imaging of structures, using low and medium magnifications [9].

A basic OCT system is consisted by reference mirror, scanning optics, A/D converter, computer and displayers, photo-detector and so on. At the heart of the system is an interferometer which is illuminated by a light source. Different beams generate interferometry and OCT captures the subsurface images from the tissues by calculating the parameters.

We will discuss OCT principles, structures and how it works to generate images in Chapter 3.

1.2.3 OCT Images

OCT images are made by OCT systems. They are the slices from 3D-scan of OCT. The colors are artificially made in order to show different structures and tissues. OCT images have speckle noise. Even there are some ways of reducing the deleterious effects of speckle on OCT imaging, the noise cannot be removed completely. That is why we have to do some processing on OCT images to make them clear.

1.3 Digital Image Processing and Image Enhancement

In this section, we will talk about the concepts of image processing and image enhancement.

1.3.1 Digital Image Processing

In Digital Image Processing, an image can be defined as a two-dimensional function $f(x, y)$, where x and y are spatial (plane) coordinates, and f represents the intensity or gray level at (x, y) point in the image. When x , y and the amplitude values of f are all finite, discrete quantities, we call the image a digital image [1].

The field of digital image processing refers to processing digital images by means of a digital computer. The digital images are composed of finite number of elements. Each of the elements has a particular location and value. These elements are

referred to as picture elements, image elements and pixels. Digital image processing is now being used in a vast area and is developing very fast. For example, it is used in Optical Coherence Tomography, X-Ray Imaging, microwave band and so on [1].

The objective of image enhancement is to process images in order to make the images more suitable for a specific application than the original images. For example, here in my research, we are more interested in the horizontal lines. Image enhancement methods have two categories: spatial domain methods and frequency domain methods. In this thesis, the wavelet algorithm used belongs to the set of frequency domain methods; and the other two algorithms belong to the set of spatial domain methods [1].

There are several steps of image processing, as shown in Fig 1.2. The first process is image acquisition. It involves preprocessing, such as scaling. Image enhancement is the simplest and most appealing areas of digital image processing. Image restoration is an area that also deals with improving the appearance of an image. Color image processing is an area that has been gaining in importance because of the significant increase in the use of digital images over the Internet. Image compression deals with techniques for reducing the storage space required to save an image or the bandwidth required to transmit it. Segmentation procedures partition an image into its constituent parts or objects. Recognition is the process that assigns a label to an object based on its descriptors [1].

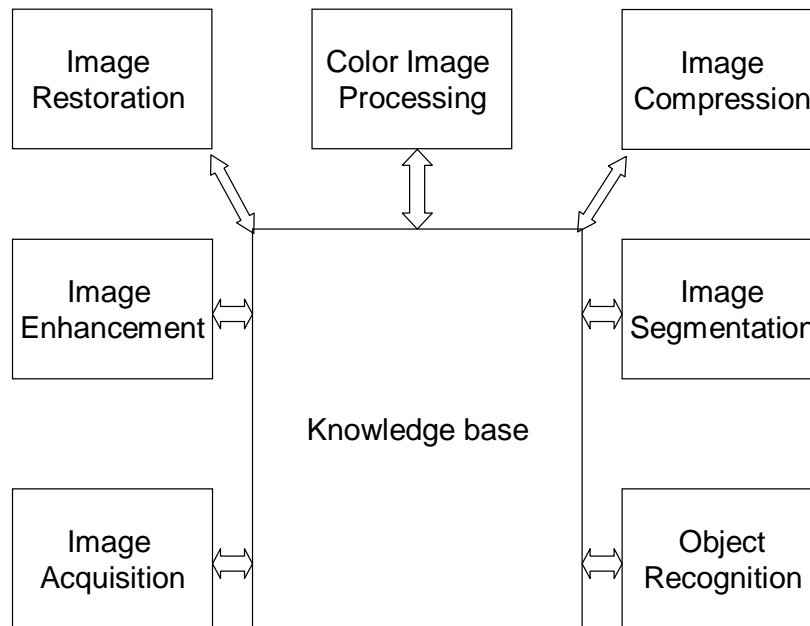


Figure 1.2 Fundamental steps in digital image processing [1]

1.3.2 Image Enhancement and Methods [1]

The idea of image enhancement is to bring out detail that is obscured, or to highlight certain features of interest in an image. An example of enhancement is when we increase the contrast of an image because it looks better for us. Enhancement is a very subjective area of image processing.

Image enhancement approaches fall into two broad categories: spatial domain methods and frequency domain methods.

Spatial domain methods include: log transformation to enhance images; spatial filters such as Gaussian filters, Laplace filters, and so on; Power-law transformations; Histogram processing such as equalization, matching; Masks; Image averaging; and combined these methods.

Frequency domain methods include: Fourier Transform; Filters in frequency domain; Homomorphic filtering and so on.

1.3.3 Enhancement Methods Used in Glaucoma Images

In this research, wavelet enhancement belongs to the frequency domain and the other two are spatial domain methods. The technique of wavelet enhancement is based on wavelet decomposition in order to separate the RGB images to four parts, each with particular coefficients. By changing some coefficients and reconstructing the parts and performing inverse transform we create new images. The wavelet process consists of a broad frequency range.

In the Sobel algorithm, since the glaucoma images are mostly composed of low frequency data, we need to emphasize high frequencies in order to enhance the edges in the image. However, some low frequencies and high frequencies are noises and cannot be removed at all. Then we combined high pass and low pass filters, that is, the Sobel filter

and the blurring filter. The two filters together can remove most of the unwanted information which do not define the edges.

Contrast adjustment in YCbCr color space is a method to maintain the color information. Transferring the RGB image to YCbCr color space and adjust the contrast of the Y component of the image to construct a new image.

1.4 Information Theory in the Analysis of the Images

After applying image enhancement algorithms to enhance the glaucoma images, the researcher will find some standard statistic of data as a reference for finding the usages and the relationships of the algorithms and the trends of the sequential images.

According to the information theory book [14], the information entropy is a measure of the uncertainty associated with a random variable. Here, images can be considered to be the random variable array, and we can use the entropy to obtain the standard measurement of how much information (uncertainties) in the images. We assume that processed images will have less entropy than the original image because the image processing algorithms will remove some useless information and some of the noises from the image. For sequential images, we can consider if the entropy of an image is lower than another image, the areas of the tissues may be smaller, which has great relationships with the health level of the patient.

According to [14], the relative entropy is a measure of the distance between two distributions. We use it to be a measurement of the relationship of two images. Mutual information of two random variables is a quantity that measures the mutual dependence of the two variables [14]. Here the researcher uses them to find the relationships between the different algorithms and the original images, for example, trying to use statistic methods to find the essences of the images. The most important usages, relative entropy and mutual information can tell us the trends of the sequential images taken from the same patient.

CHAPTER 2

LITERATURE REVIEW

In this chapter we present a summary of the necessary literature reviewed in support of this thesis. Where required, discussions are included concerning how the literature references are used in this research.

2.1 Image Enhancement Algorithms Used in Glaucoma Images

Even if there are a lot of image processing books, we still believe Gonzalez's book [1] is an eternal classic book. It contains most of the basic knowledge and methods in image processing field. In this book, the author gave us basic methods in image enhancement in the spatial and frequency domain. We tried most of them but the results were not satisfactory. The images have more low frequencies than high frequencies.

Gonzalez [3] described intensity transformation function method to enhance images. However, that method is also very useful for gray scale images. In order to use it in color images, we changed RGB images to YCbCr color space and applied intensity transformation function to the Y component and reconstructed the image using the new Y and other components.

Gonzalez [3] also described wavelet transform in two dimensions. He mentioned wavelet decomposition filters and decomposition coefficients (A=approximation coefficients, H = horizontal detail coefficients, V = vertical detail coefficients, D = diagonal detail coefficients [5], see Chapter 3 and equation 3.2). We can make the image smooth by changing the coefficients.

It is very common to use wavelet to do image coding and using wavelet decomposition to obtain different coefficients. But using wavelet theory and methods to do image enhancement is not very common.

Based on Gonzalez's two books [3] and [1], we created a wavelet enhancement method. We calculated the coefficients by using wavelet decomposition and set the horizontal detailed coefficients (see Chapter 3) to zero. This action allowed us to keep the color and other details of the images.

In the books, Gonzalez described spatial enhancement methods by using filters. Though the Sobel operator is commonly used, we have to combine it with another filter in order to create a new method.

2.2 Principle of OCT

Since the glaucoma images are scanned by OCT, the theory and structures of OCT are also very significant in this research. Joseph M. Schmitt [11] has described the basic theory and structures. The most important characteristic of OCT is interference. By using interference, OCT can calculate the data of the object and extract the 3D information. Computer processing can help to create higher quality images.

Chien-Wen Chang [9] describes the time domain OCT and frequency domain OCT very clearly. In the time domain OCT, the calculations are implemented by processing the interference of two partially coherent light beams from the source intensity. Then different coefficients are calculated which are used to compute the complex degree of coherence. Finally, the Doppler-shifted optical carrier is calculated, which gives the coherence length of the source and the axial resolution of the OCT. By using special equipment to send the data to computer, computers can generate digital images [9].

The frequency domain OCT is more popular nowadays than time domain OCT. That is because the Inverse Fourier Transform (IFT) provides depth-scan of the spectrum of the backscattered light from the object.

The spectrum interferogram is Fast Fourier Transform (FFT) into the time domain coordinates to reconstruct the frequency function $H(\omega)$. After simulating the system interference result from the light source and the object structure, we have the

interference signal of frequency domain. By transforming the frequency spectra and get the sample internal distribution for one dimension imaging. The output intensity spectrum corresponds to an intensity measurement at each detector. Computers are used to calculate those data and create images[9].

In the Hand book of Optical Coherence Tomography [10], the author describes how to generate artificial color images. The frame grabber comprise A/D converter and A.D converter can help changing the signal to digital data and send them to a computer.

Joseph M. Schmitt [11] mentions there are a lot of speckles in OCT images. Most models of OCT wash away speckle by averaging the spatial properties of the tissues in the computation of the interference signal. But this kind of averaging is not possible in practice. There is a close connection between speckle generation and the optical band-pass response of OCT imaging systems, and it makes the signal-carrying and signal-degrading roles of speckle very hard to distinguish. So we have to do image enhancement and remove some noise [11].

2.3 Glaucoma

Having sufficient knowledge of glaucoma can help me analysis the glaucoma images. Therefore this section discusses some fundamental background about the disease (glaucoma).

Glaucoma [13] is a group of diseases of the optic nerve involving loss of retinal ganglion cells in a characteristic pattern of optic neuropathy. Glaucoma will lead to permanent damage of the optic nerve and will lead to blindness [13].

Glaucoma is the second eye disease to bring blindness in USA. However, it can be prevented. So let everybody knows about glaucoma and how to prevent it is very significant event in US. The OCT scanned glaucoma images are not perfect for doctors to use in diagnosis. Consequently, image processing techniques applied can greatly help to get better diagnosis.

2.4 Information Theory

In [14], Thomas M. Cover and Joy A. Thomas describe the basic knowledge of information theory including entropy, mutual information and relative entropy.

Applications of the mutual information are given in [14]. For example, mutual information can be used in medical imaging for image registration. Given a reference image and a second image that is defined in the same coordinate system as the reference image, the process could be to deform the image until we find the maximum mutual information between the original image and the reference image. This process can be used to track common characteristics between the images as to note some differences between them. It can also be used in the embedded theorem, for HMM (Hidden Markov Model) and for comparing data clusters.

The recent article [12] discussed methods and results of applying mutual information in image registration. The reported results in [12] are very good. Since information theory is used more and more in image processing, we employ it in the analysis of the image enhancement results. The information theory results tell us which two images are more related and more similar.

2.5 Research Questions

Dr. Hylton Mayer (Professor in the Medical School at Yale University) indicated in his email correspondence that doctors would like programs and processes that highlight different layers of the retina and to show where pathologies are. Figure 2.1 shows a cross reference anatomical microscopic image of the human eye. The image (Figure 2.2) shows the nerve fiber layer, the inner nuclear layer, the outer nuclear layer, and the RPE/pigmented cell layer.

An OCT of a glaucoma image of such a layered structure is shown in Figure 2.2. Our analysis will be performed on colored OCT images similar to Figure 2.2.

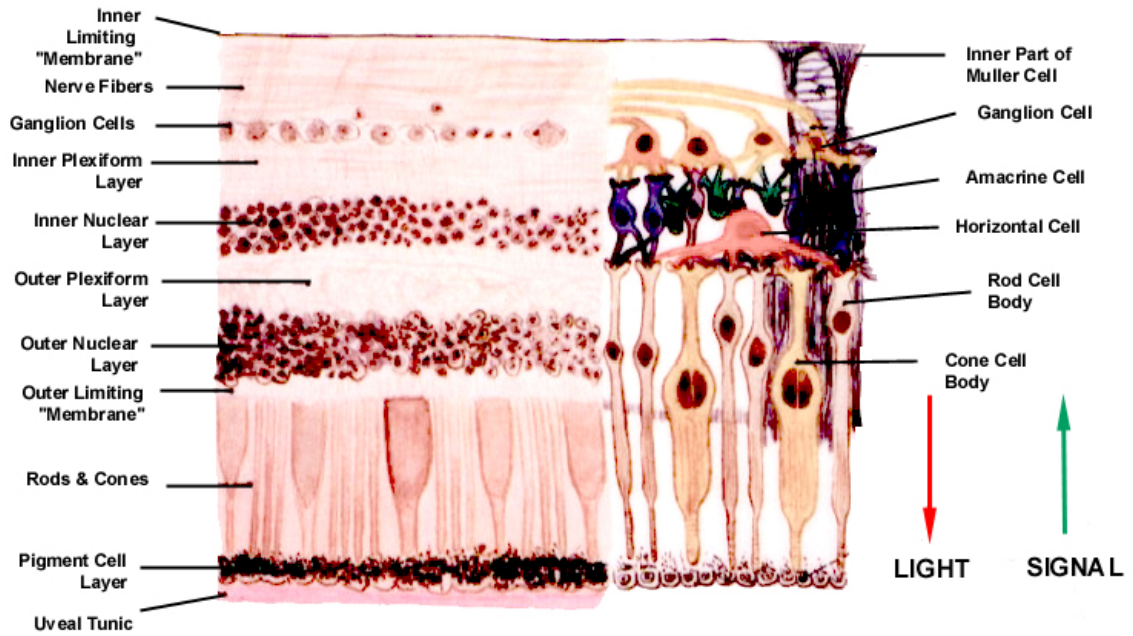


Figure 2.1 The cross sectional image

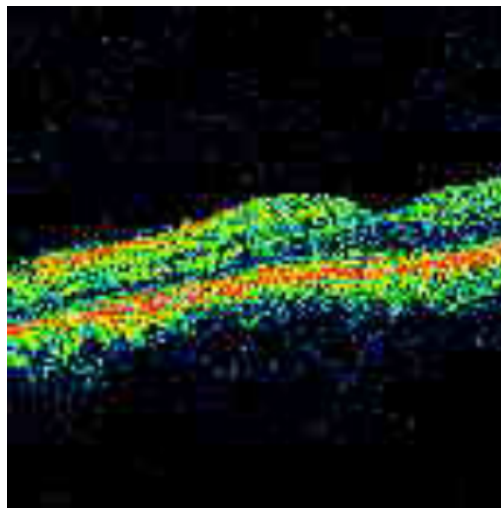


Figure 2.2 Glaucoma image (macular) scanned by OCT

In every glaucoma image (Glaucoma images scanned by OCT), different colors represent different structures and tissues in the back of the eye as mentioned above.

Enhancement of the images emphasizes horizontal layers structures. These enhanced structures provide doctors with information containing the distances between two edges of the structures in the images in effect whether the patient eyes are healthy or whether there are signs of glaucoma. Hence, this research is to find a method to help doctors better measure the distances between lines in the OCT images.

Therefore, the research questions are:

1. Can the tissue structures of the human eye as shown in an OCT image be enhanced to emphasize the layered structures that represent the tissue layers?
2. Can analytical methods from information theory be used to aid doctors in extracting needed diagnostic information from the enhanced OCT images?

To deal with the first research question is a process to understand the special composition of OCT images. According to [3], [1] and the FFT (Fast Fourier Transform), this image (Figure 2.2) are composed of both low frequencies and high frequencies. The edges of the well defined tissue structures are high frequencies. However, the effects to remove the low and high frequency noises will remove important structure information. So how to remove the noise and enhance the useful information of structures and also keep the color information of the images, is a very big and significant topic in this research. The image enhancement algorithms must be chosen carefully to achieve this goal. That is, to remove noise, to enhance the structures and to improve diagnosis for doctors.

In Chapter 3, we provide the details of the image enhancement algorithms and their selection criteria. We will also provide the methods of information theory used in this research.

CHAPTER 3

ALGORITHMS USED ON GLAUCOMA IMAGES

In this chapter, we will introduce the enhancement algorithms used to process the glaucoma images, the mathematical theory of the algorithms, the theory of OCT (Optical Coherence Tomography) and the theory and methods of information theory.

3.1 The Enhancement Algorithms

In this section, we discuss the image enhancement algorithms used to process the glaucoma images. There are three algorithms: Wavelet decomposition and enhancement algorithm; Sobel enhancement algorithm and Contrast adjustment algorithm.

3.1.1 Wavelet Algorithm

The wavelet is a mathematical function and method which can divide signals into different frequency components. The wavelet transform is used to represent to signals or functions with wavelets [2].

In this case, we used the wavelet decomposition of discrete wavelet transform to decompose the image into 4 parts: approximation matrix cA (see equation 3.2), details matrices cH , cV , and cD (horizontal, vertical, and diagonal). The definitions and details will be represented in section 3.2. The steps are shown below:

1. Change the image from RGB color space to HSV color space. In the RGB model, each color is represented by its primary spectral components of red, green and blue [1]. In HSV color space, images are decomposed to three parts: hue, saturation and value.

2. Use Value component in HSV color space and do wavelet decomposition. After that we get four coefficients: cA , cH , cV and cD .

3. We can find that the horizontal lines are the most important information. Based on this, set cV and cD to be zero in order to enhance the horizontal information.

4. Filter cA part using Gaussian filter (high pass filter) can give us sharper image. We do this step twice to enhance the effect (see Matlab code in Appendix A).

Reconstruct the image (see Figure 3.1). A flow chart of the wavelet algorithm is given in Figure 3.1:

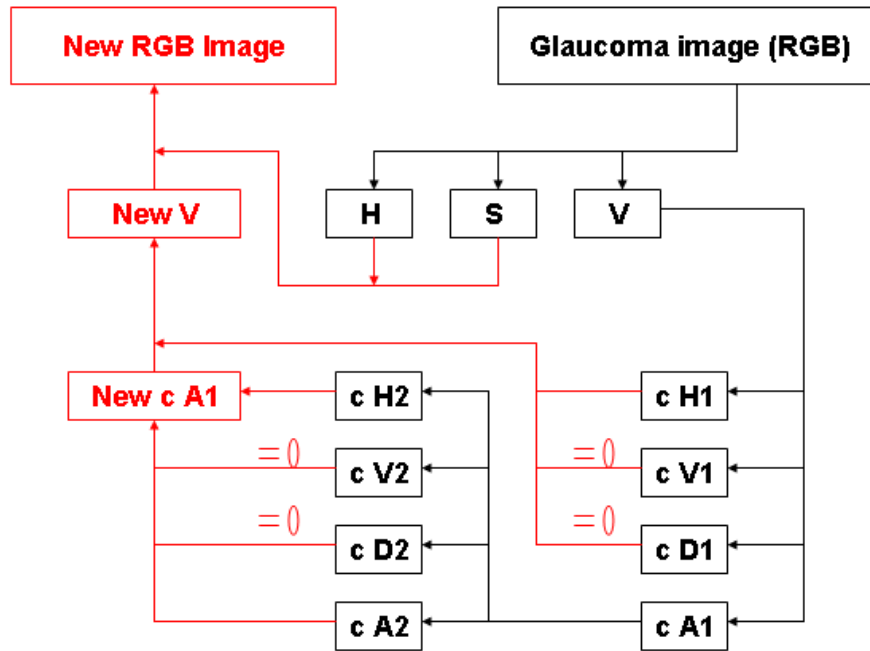


Figure 3.1 The flow chart for the wavelet algorithm

3.1.2 Sobel Algorithm (Sobel Filter and Blurring Filter)

The researcher believes that the Sobel method/ Sobel operator is pretty efficient in determining the high gradient drops in images, because Sobel operator is essentially a high pass filter which can determine the lines and edges of the images.

The Sobel method is basically used to detect edges in an image because Sobel operator is a useful method to calculate the gradient. Sobel operator is represented as masks of even sizes, for example, we are interested in the 3*3 size masks. As we can see from Figure 3.2 (Sobel operator), the left Sobel operator, the difference between the first and the third rows of the 3*3 image region will approximates the derivative in the x-

direction, and in the right Sobel operator, the difference between the first and the third columns will appreciate the derivative in the y-direction. These are Sobel operators. In this research, we use an x-direction Sobel operator which can detect the edges and enhance the edges of the horizontal lines [1].

-1	-2	-1
0	0	0
1	2	1

-1	0	1
-2	0	2
-1	0	1

Figure 3.2 Sobel operators

In this research we used the Sobel operator to convolve the image with a small filter in the horizontal direction since we needed to make the horizontal lines of the image clearer. The original image has several horizontal lines that are indistinguishable from each other. The resulting image shows the distinct horizontal lines that are present in the original image. In other words, after using the Sobel operator we can see the horizontal lines clearly in the resulting image. However, we believe the resulting image contains a lot of high frequency noise. This can be improved by applying a low pass filter on the resulting image which will eliminate all high frequency noise making the image clearer. The researcher chose the blurring filter, which destroys detail and sharp edges. A flow chart of the Sobel algorithm is given in Figure 3.3:

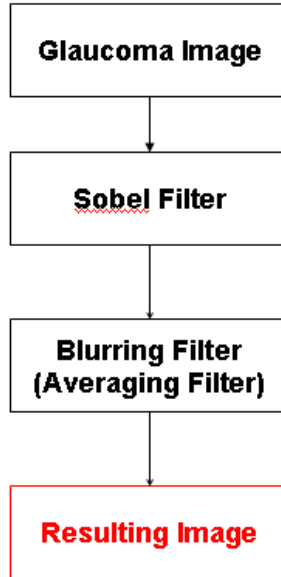


Figure 3.3 The flow chart for the Sobel algorithm

3.1.3 Contrast Adjustment Algorithm

We use this contrast adjustment algorithm based on YCbCr color space. The YCbCr color space has been widely used in digital video these years. YCbCr color space contains luminance information which is represented by component Y, and color information is represented by two color-difference components Cb and Cr. Component Cb is the difference between the blue component and a reference value, and component Cr is the difference between the red component and a reference value [3].

Here we chose to use YCbCr color space in order to maintain the color information from the Y part. Change the RGB image to a YCbCr image as part of the contrast algorithm, and then take the Y part and map the intensity values of the image to

new values. These actions enhance the contrast of the image. Finally, integrate the enhanced Y part back into the image.

A flow chart of the contrast adjustment algorithm is shown in Figure 3.4:

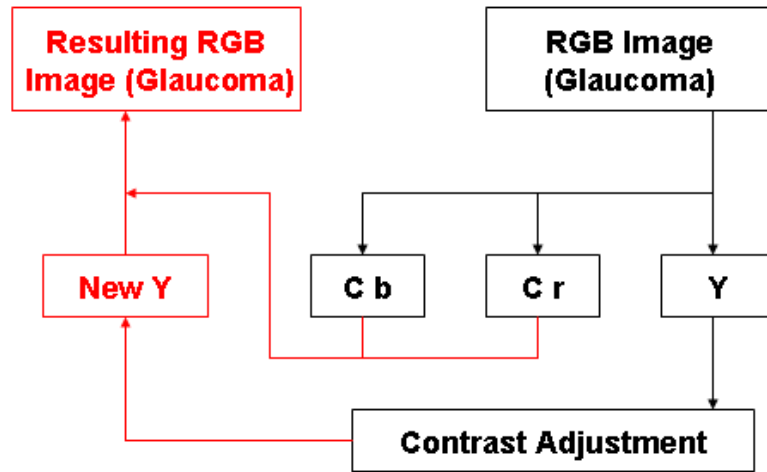


Figure 3.4 The flow chart for the contrast adjustment algorithm

3.2 Mathematics in the Algorithms, OCT and Information Theory

In this section, we will describe the mathematical bases of the three algorithms. Since the images are all obtained by OCT, we will include some theory and principles of OCT, as an effort to make the thesis self-supporting. Finally, we will present some details of information theory and some applications of its methods.

3.2.1 Mathematics in Enhancement Algorithms

In this section, we will describe the mathematical bases of each image enhancement algorithm we used in this research.

3.2.1a Wavelet Decomposition in Wavelet Algorithm

In this section, we will introduce the mathematics in wavelet algorithm. Wavelet decomposition is the most important part in this algorithm.

a. Definition of DWT

First of all, we have to be clear about the basic definition of DWT. The resulting coefficients from samples of a continuous function after we apply wavelet transform are called a discrete wavelet transform (DWT).

The DWT of a signal x is calculated by passing it through a series of filters. The sampled signal is decomposed by a low pass filter with impulse response g . The resulting signal is the convolution of g and the signal [1]:

$$y[n] = (x * g)[n] = \sum_{k=-\infty}^{\infty} x[k]g[n-k] \quad (3.1)$$

The signal is also decomposed simultaneously by a high-pass filter h . The resulting signals give the detail coefficients from the application of the high-pass filter

and approximation coefficients from the application of the low-pass filter [1]. We will show details about the applications in the next section.

b. Matlab Algorithm

This researcher used Matlab command “dwt2” to decompose the image signals, which is based on the basic idea of DWT. “This command performs a single-level two-dimensional wavelet decomposition with respect to either a particular wavelet ('wname') or particular wavelet decomposition filters” [5].

$$[cA, cH, cV, cD] = dwt2('wname') \quad (3.2)$$

Equation 3.2 calculates the approximation coefficients matrix cA and details coefficients matrices cH , cV , and cD (horizontal, vertical, and diagonal, respectively) of the input image. The 'wname' string contains a kind of a wavelet name, for example, Haar, DB [5]. The following chart describes the basic decomposition steps:

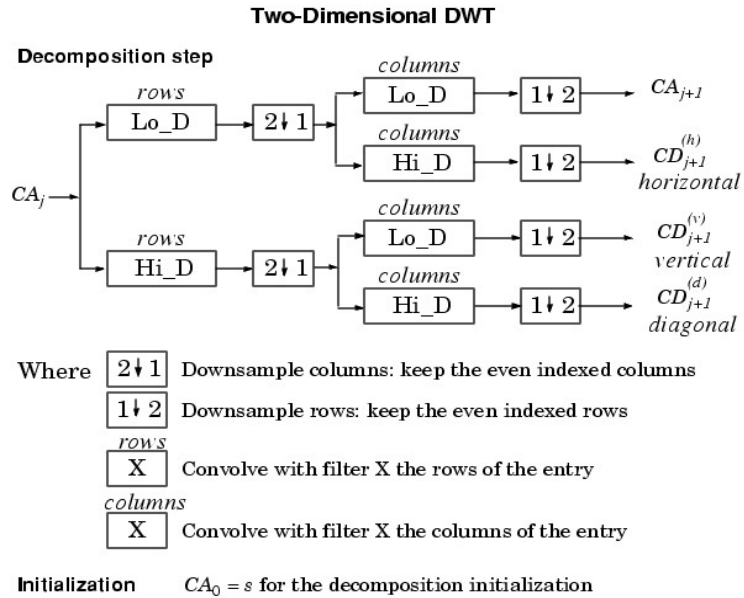


Figure 3.5 2D DWT of Matlab Algorithm [5]

Here in this wavelet algorithm, we used the wavelet to decompose the image to four parts: approximation matrix cA , details matrices cH , cV , and cD (horizontal, vertical, and diagonal). The researcher used Haar wavelet.

The Haar wavelet is a certain sequence of functions (see Figure 3.6). The Haar wavelet is the simplest and oldest wavelet [1].

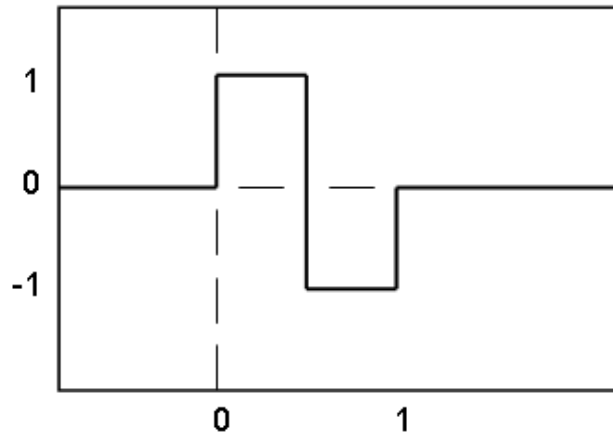


Figure 3.6 The Haar wavelet $\psi(x)$ [1]

The Haar wavelet's mother wavelet function $\psi(x)$ can be described as[1]

$$\psi(x) = \begin{cases} 1 & 0 \leq x < 0.5 \\ -1 & 0.5 \leq x < 1 \\ 0 & \text{elsewhere} \end{cases} \quad (3.3)$$

The wavelet algorithm steps are described before. Here we described again: Set a Gaussian filter (a high pass filter) and filter the image; change the image to HSV color space. Use wavelet method to decompose filtered V to cA, cH, cV and cD; set cV and cD to be zero to enhance the result and use the filter to filter cA component. Follow this step twice; take the filtered cA back to the image to do reconstruction.

From the mathematics of wavelet algorithm, we can be sure that enhancement of certain parts of wavelet decomposition will enhance the horizontal lines of the OCT

images and since some detailed components are removed, the images will become slightly blurred.

3.2.1b Sobel Operator in Sobel Algorithm

In mathematics, the gradient of an image $f(x,y)$ at location (x,y) is defined as the vector G_x and G_y (see equation 3.4 and 3.5) [1].

From the Figure 3.2, we calculate G_x and G_y by:

$$G_x = (z_7 + 2z_8 + z_9) - (z_1 + 2z_2 + z_3) \quad (3.4)$$

$$G_y = (z_3 + 2z_6 + z_9) - (z_1 + 2z_4 + z_7) \quad (3.5)$$

The gradient G is calculated by the equation:

$$G = \sqrt{G_x^2 + G_y^2} \quad (3.6)$$

We can also calculate the gradient's direction [1]:

$$\Theta = \arctan\left(\frac{G_y}{G_x}\right) \quad (3.7)$$

Where, Θ is 0 for a vertical edge which is darker on the left side [1].

Therefore, we are clear that using Sobel operator to filter the image, we will obtain “sharp” images.

The researcher created blurring filter by herself. First we create a matrix which has the size larger than the original image, for example, if the original image has the size n by n , the matrix has the size of $(n+2)$ by $(n+2)$. Evaluate the edges of the matrix by the edge values of the original image and evaluate the middle part (the same size as the original image) by the intensities of the original image (see Appendix A for Matlab code). Filter this new matrix by an averaging filter, then cut the middle part which have the same size as the original image. The process is applied by different channels (red, green and blue). Here, the blurring filter is mainly created by the averaging filter.

Now we describe the mathematics of an averaging filter. The response of a smoothing, linear spatial filter is simply the average of the pixels contained in the neighborhood of the filter mask. These filters are called averaging filters [1].

By replacing the value of every pixel in an image by the average of the gray levels in the neighborhood defined by the filter mask, this process results in an image with reduced “sharp” transitions in gray levels [1].

Because random noise typically consists of sharp transitions in gray levels, the most obvious application of smoothing is noise reduced. But the edges are characterized by sharp transitions in gray levels, so averaging filter will blur edges. The 3×3 smoothing filter we used in Sobel algorithm is shown below [1]

$$0.11 \times \begin{array}{|c|c|c|} \hline 1 & 1 & 1 \\ \hline 1 & 1 & 1 \\ \hline 1 & 1 & 1 \\ \hline \end{array}$$

Figure 3.7 The averaging filter used in this Sobel algorithm

Since the averaging filter (blurring filter) is a low pass filter and will blur the edges, Sobel filter is a high pass filter and will make the edges clearer, we combined the two and created a band pass filter, which will remove some of the background noise, the tissues between the lines and the enhance the lines.

3.2.1c YCbCr Color Space and Contrast Adjustment

Researcher also used another color space, YCbCr color space to enhance the images. The YCbCr color space is used widely in digital video. In this format, luminance information is represented by a single component, Y and color information is stored as two color-difference components, Cb and Cr. The relationship of RGB and YCbCr is [3]:

$$\begin{bmatrix} Y \\ Cb \\ Cr \end{bmatrix} = \begin{bmatrix} 16 \\ 128 \\ 128 \end{bmatrix} + \begin{bmatrix} 65.481 & 128.553 & 24.966 \\ -37.797 & -74.203 & 112.000 \\ 112.000 & -93.786 & -8.214 \end{bmatrix} \begin{bmatrix} R \\ G \\ B \end{bmatrix} \quad (3.8)$$

$$J = imadjust(I,[low_in;high_in],[low_out;high_out], gamma) \quad (3.9)$$

There is a Matlab command “imadjust” to change the adjustment of the images. Equation 3.9 [5] maps the values in I to new values in J. Gamma specifies the shape of the curve which describe the relationship between I and J. If gamma is less than 1, the mapping will give higher (brighter) output values. If gamma is greater than 1, the mapping will give lower (darker) output values [5]. Here in this algorithm, researcher chose 1.8, which will make the images darker.

Now we are clear that by changing the contrast of the image, even though the image will be darker, some parts will be more obvious.

3.2.2 Mathematics in Information Theory

In order to make this section complete, we will provide the background of information theory. First we define Entropy, second is relative entropy, finally we define mutual information.

3.2.2a Entropy

“In information theory, entropy is a measure of the uncertainty of a random variable. All of the entropy values will be measured in bits.” [14].

The entropy of a discrete random variable X with a probability mass function $p(x)$ is defined by [14]

$$H(X) = -\sum_x p(x) \log_2 p(x) \quad (3.10)$$

Since entropy can show the uncertainty of the random variables, it of course can show the uncertainty of the images. We suppose processed images have less entropy than the original one. That is because the image processing algorithms will remove some useless information and the noises from the original images. Then we will calculate the entropy of each line of the original images and processed images, trying to have more data to analyze.

3.2.2b Relative Entropy

“The relative entropy is a measure of the distance between two distributions. The relative entropy is a measure of the inefficiency of assuming that the distribution is q when the true distribution is p .” [14]

The relative entropy between two probability mass function $p(x)$ and $q(x)$ (or two random variables) is defined as [14]

$$D(p\|q) = \sum_{x \in \mathcal{X}} p(x) \log \frac{p(x)}{q(x)} \quad (3.11)$$

Since relative entropy can represent the relationship of two images, researcher calculated it in order to find how related in the images and which two are more related.

To summarize the discussion, we will discuss the three methods used in calculating the relative entropy.

Method 1. Matrix of Probability

This method is based on the definition of matrix of probabilities in paper “*Improving the Entropy Algorithm with Image Segmentation*” [12], we firstly develop the matrix of probabilities of each image and then calculate the relative entropy of each corresponding pairs of pixels which have the same position of the images. Finally, we sum the set of relative entropies for the complete images. The difference from [12] is, we calculate the probability of each pixel using

$$p(n) = (\sum \text{occurrences of } n \text{ in } M) / (\sum \text{pixels in } M) \quad (3.12)$$

Method 2. Probability matrix based on Histograms

This method is based on the histograms. Find out the histograms of the intensities in the images then normalized them using equation (3.12). Use these probability vector based on the histogram and calculate the relative entropy then sum them as we did in Method 1. There is a condition that we should move out all of the zeros in histograms.

Method 3. Using Different Conditions

Method 3 is almost the same as Method 2. Researcher used different conditions in Method 2 and Method 3. In Method 2, since the probability cannot be zero when calculating relative entropy, we removed every zero probability in the four probability matrices. In Method 3, I only removed every zero in every pair of probability matrix.

For example, for the different images we have the probability vectors p_1 , p_2 , and p_3 . In Method 2, if $p_1(5)$ is zero, we will set $p_2(5)$ and $p_3(5)$ to be zero, no matter if they are equal to zero. But in Method 3, we set $p_2(5)$ to be zero only when we compare p_1 and p_2 , it has nothing to do with p_3 at this situation.

The reason researcher used matrix of probabilities to calculate relative entropy in Method 1 is, it contains the position information since every pixel is substituted by its probability. And because every element is probability, which is between 0 and 1, we can use this matrix of probability to calculate relative entropy to find a “reference” value, not a true value.

3.2.2c Mutual Information

The Mutual information is a measure of the dependence between the two random variables. It is symmetric in the two random variables and always nonnegative [14].

For two random variables X and Y, the mutual information is defined by [14]

$$I(X;Y) = H(X) - H(X|Y) = \sum_{x,y} p(x,y) \log \frac{p(x,y)}{p(x)p(y)} \quad (3.13)$$

Mutual information can represent the relationship and the fitness between the two images. However, to calculate the mutual information is very difficult. We probability cannot calculate the joint entropy, because we don't know the joint probabilities and given probabilities. But in the paper [12], the author pointed out that if we calculate the maximum area value, that is equal to the work we calculate the mutual information. That will be more convenient.

In this paper, the author gives us an effective algorithm based on the mutual information. The steps of calculation of mutual information [12]:

Step 1: Calculate Probability for Each Pixel and Weight Value

The calculation of the weight probability for each pixel value for an image M using equation 3.14 [12]:

$$p(n) = 1 - (\sum \text{occurrences of } n \text{ in } M) / (\sum \text{pixels in } M) \quad (3.14)$$

Step 2: Distribute Probability to Pixels

Each occurrence of a pixel intensity value should be replaced with its probability of occurrence in a new matrix with size corresponding to the image size.

Step 3: Calculate the Maximum Area

The maximum resulting area value corresponds to the position of the maximum mutual information.

In this research, researcher used two methods to calculate the mutual information. **Method 4** is following the same steps as we listed above.

Method 5 contains transformation. We can see from the glaucoma images, the positions of the structures are different in an image axis, meaning that some structures are higher in the black background of glaucoma images and some are not. Even if the two images are very similar, they may have small values of the overlap area which correspond to mutual information because of differences in positions.

Therefore, changing positions to move the structures down one row by one row in the image (we call it transformation) and calculating the overlap area of each changed position, consider the maximum area value is corresponding to the right positions. This

researcher believes this way is more reasonable and accurate. The calculation of the overlap areas is the same as the steps in Method 4.

3.2.3 Correlation Analysis

In this section, we will discuss the definition and mathematics of correlation.

3.2.3a Definition of Correlation

In probability theory and statistics, correlation indicates if the two random variables are independent or vary together [10]. So we decided to use correlation to find the relationships among these images, in order to know if they were from the same patient.

3.2.3b Mathematical Properties

“The coefficient of correlation describes the strength of the relationship between two sets of interval-scaled or ratio-scaled variables”. The correlation coefficient r between two random variables X and Y is defined as the following formula [10]:

$$r = \frac{E(XY) - E(X)E(Y)}{\sqrt{E(X^2) - E^2(X)}\sqrt{E(Y^2) - E^2(Y)}} \quad (3.15)$$

The correlation coefficient 1 or -1 means perfect correlation. The closer the coefficient is to 1 or -1, the stronger the correlation between the two variables. If the variables are independent, the correlation coefficient will be 0 [10].

Therefore, we chose to use correlation to determine the relationships between the images.

3.2.4 Mathematics in Optical coherence tomography (OCT)

In this research, all images are taken by OCT, therefore, the theory of operation and the mathematical knowledge of OCT. Optical techniques are very important in biological medicine. The technology is safe, cheap and offer a therapeutic potential in many areas[9]. For example, OCT can provide more information than MRI (Magnetic Resonance Imaging).

3.2.4a Interferometry Principle

In essential theory and background of OCT are taken from these references: [8], [9], [10],[11].

“Interferometry is the technique which can diagnosis the properties of at least two waves by acquire the information from the pattern of interference generated by their superposition”[8].

OCT is based on low coherence interferometry between a split and later re-combined broadband optical field. The split field travels in a reference path, and reflects from a reference mirror and also in a sample path. Due to the broadband light source, the interference between the optical fields is observed when the reference and sample arm optical path lengths are matched, in order to within the coherence length of the broadband light. We express the electric field $E(\omega, t)$ as a complex exponential [9]:

$$E_{in}(\omega, t) = s(\omega) \exp[-i(\omega t + kz)] \quad (3.16)$$

$s(\omega)$: The source field amplitude spectrum. ω : frequency. t : time variation. k : wave-number. z : distance.

We know the input phase is arbitrary, and the interferometry only measures the relative output phase between the two paths, the phase term can be dropped from the input electric field, as we can see from the following Figure 3.8.

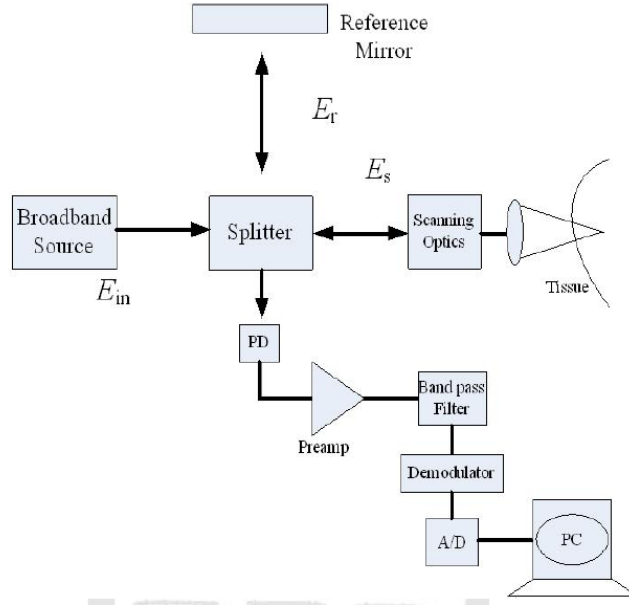


Figure 3.8 Block diagram of an OCT system [9]

The reference mirror is considered to be ideal and the beam splitter has reference and sample arm intensity transmittance γ_r and γ_s . The frequency domain response function $H(\omega)$ can describes its internal structure and account for phase accumulation, and also describes the overall reflection from all structures distributed in the z direction within the sample [9]:

$$H(\omega) = \int_{-\infty}^{\infty} r(\omega, z) e^{i2n(\omega, z)d/c} dz \quad (3.17)$$

A sample layered sample can be modeled by writing the continuous sample integral, as a summation over N individual layers and assuming negligible dispersion and losses [9]:

$$H(\omega) = \sum_{j=1}^N r_j \exp[i2 \frac{\omega}{c} \sum_{m=1}^j n_m d_m] \quad (3.18)$$

D_m : the physical thickness of the m th layer, with a refractive index n_m . The reflectivity of each layer r_j , assuming that the light is perpendicular to each layer [9]:

$$r_j = (n_{j+1} - n_j) / (n_{j+1} + n_j) \quad (3.19)$$

After calculation, the frequency and path difference dependent intensity will be expressed as[9]:

$$I(\omega, \Delta z) = \gamma_r \gamma_s S(\omega) |H(\omega)|^2 + \gamma_r \gamma_s S(\omega) + 2\gamma_r \gamma_s \text{Re}[S(\omega)H(\omega) \exp(-\psi(\Delta z))] \quad (3.20)$$

The first two terms are the mean (dc) intensities returning from the reference and sample arms of the interferometers. The nature of the interference fringes depends on the degree to which the temporal or spatial characteristics of E_r and E_s match and the visibility of interference fringes can be given by [9]:

$$V = [I_{\max} - I_{\min}] / [I_{\max} + I_{\min}] \quad (3.21)$$

3.2.4b Time Domain OCT

There are two categories of OCT: Time-domain OCT (TD-OCT) and Frequency-domain OCT (FD-OCT). In this research, the images are generated from time domain OCT.

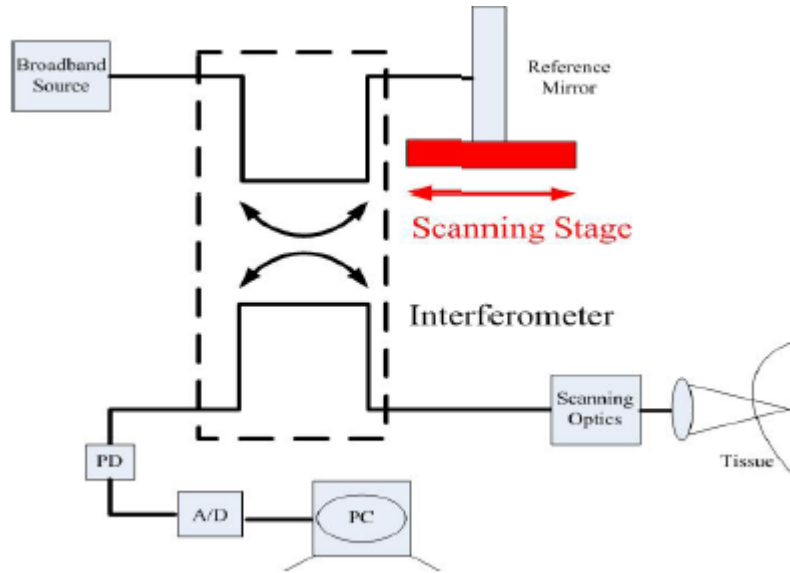


Figure 3.9 The basic block diagram of the TD-OCT

Time domain OCT is based on the variable path of scanning stage for time domain demodulation. The light sources pass through a beam splitter and are split into two beams, one beam will pass to reflective mirror and another beam is passed to the sample arm (see Figure 3.9). Finally the two light beams combined together and are received by the optical detector [9]. Figure shows the basic structures of an TD-OCT.

We can calculate the output power of the Gaussian spectral density light source, and therefore the interference of OCT system can be calculated by [9]:

$$I(\Delta z) = \gamma_r \gamma_s P_{out} [1 + |H(\omega)|^2 + 2R_e[H(\omega) \exp(-\psi(\Delta z))]] \quad (22)$$

The time function signal at Photo-detector is received under the modulation of scanning stage. We simulate the OCT signal condition by setting some parameters in order to analyze the measurement process. For example, set the path length between two

mirrors is zero. After these simulation processes above, we will get the optical length of each layer and the one dimension interferogram about the sample structure. The whole process and calculation are followed by the formulas [9]:

$$\begin{aligned}
 n_m \sin(\theta_m) &= n_{air} \sin(\theta_0) = NA \\
 d_m \tan(\theta_m) &= \Delta z_m \tan(\theta_0) \\
 \Delta l_m &= n_m d_m - \Delta z_m \\
 n_m^2 &= \frac{1}{2} (NA^2 + 4(1 - NA^2)(1 + \frac{\Delta l_m}{\Delta z_m})^2)^{0.5}
 \end{aligned} \tag{3.23}$$

Where θ_m and θ_0 are an incident angle at the external surface and a refraction angle at the front surface of mth layer. NA represents the numerical aperture. This technique can provide an accurate analysis for TD-OCT. It also has some position problems and low scanning speed [9].

3.2.4c Frequency Domain OCT (FD-OCT)

In standard OCT two scans have to be performed. Only the lateral OCT scan has to be performed in the Frequency-domain technique. Depth-scan is provided by an inverse FT of the spectrum of the backscattered light from reference and sample arms. The backscattered field signals can be obtained by spectral interferometry techniques or wavelength tuning techniques. In FD-OCT setups optical energy is measured rather than optical power. It has the advantages that no moving parts are required to obtain axial scan. The reference path length is fixed, the detection system is replaced with a spectrometer or the module of diffraction grating and CCD. The spectrum interferogram

is FFT (Fast Fourier Transform) into the time domain coordinates to reconstruct the frequency function $H(\omega)$ and depth resolved sample optical structure(Figure 3.10)[9].

After simulating the system interference result for the light source and sample structure, we can get the interference signal of frequency domain(Fig 3.11(a)). The signal is the spectra interferogram distribution, we can get time interferogram distribution with Fourier transform (FT), transforming the frequency spectra and get the sample internal distribution for one dimension imaging(Fig 3.11(b))[9].

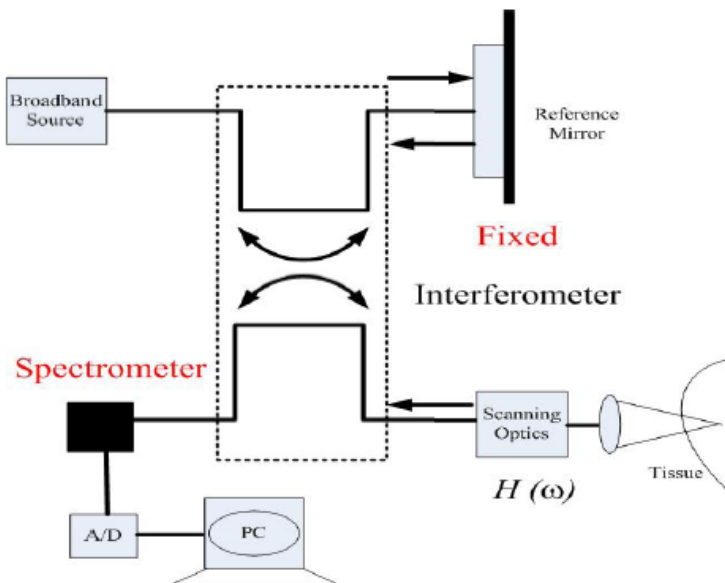


Figure 3.10 FD-OCT optical system structures [9]

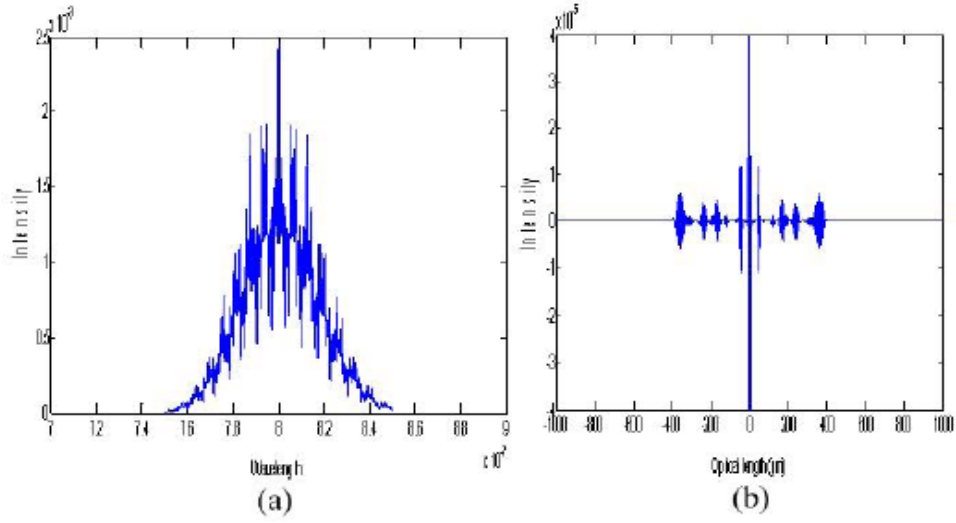


Figure 3.11 The simulation of interferogram under sample test: (a)spectrum interferogram; (b) time function interferogram [9]

In a real system, the output intensity spectrum is a set of N discrete data points, which correspond to an intensity measurement at each detector in the array. So FT can be achieved by means of FFT on a computer or hardware. FT result is composed of a series of $N/2$ discrete steps determined by the detector spectral width $\Delta\Omega$ [9]:

$$\Delta\tau = 2\pi / \Delta\Omega \quad (3.24)$$

$$\Delta\Omega = 2\pi c\Delta\lambda / \lambda^2 \quad (3.25)$$

We can converse the result into spatial domain by both sides of equation 3.24 by c/n_{ave} (n_{ave} is an assumed average sample refractive index). The maximum depth is determined by [9]:

$$z_{\max} = \lambda_0^2 N / 4n_{ave} \Delta\lambda \quad (3.26)$$

The above discussion is to modify a TD-OCT system and convert it to FD-OCT system. The FD-OCT system is more popular than TD-OCT nowadays. The FD-OCT has a lot of advantages: it has fast scanning speed, high resolution images and high system sensitivity[9].

3.2.4d Image Acquisition and Display

Frame grabbers are designed to digitize video signals. A frame grabber is always needed in an imaging system when images are displayed at video rate.

The block diagram of a simple frame grabber is shown below(Figure 3.12). The frame grabber comprise four sections: A/D converter, a programmable pixel clock, and acquisition and window control unit, and a frame buffer. Video input is digitized by the A/D converter with characteristics such as filtering, reference and offset voltages, gain, sampling rate and so on. The frequency of the programmable pixel clock determines the video input signal digitization rate or sampling rate. In addition, the acquisition and window control circuitry also controls the region of interest (ROI), whose values are determined by the user. Image data outside of the ROI are not transferred to the frame buffer and are not displayed on the screen [10].

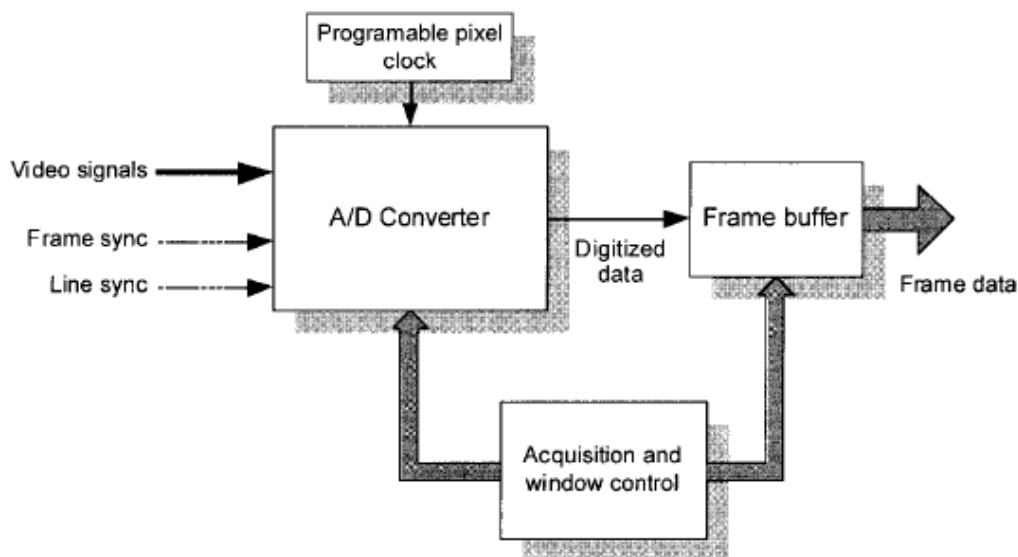


Figure 3.12 The block diagram of frame grabber

Once digitized by a conventional A/D converter or frame grabber, 2-D OCT image data representing cross-sectional or en face sample sections are typically represented as an intensity plot using gray-scale or false color mapping. The intensity plot encodes the logarithm of the detected signal amplitude as a gray-scale value or color that is plotted as a function of the two special dimensions. The choice of the color mapping used to represent OCT images has a very important effect on the perceived impact of the images and on the ease with which images can be reproduced and displayed. Many authors have used the standard linear gray scale for OCT image representation, with low signal amplitudes mapping to black and strong to white. Some groups have a reverse gray scale, with strong reflections as black on a white background. A large variety of false color maps are applied to OCT images, the most widely used are the original blue-green-yellow-red-white "retina" color scale [10].

There are a lot of speckles in OCT images. Although many researchers have observed the effects of speckle on OCT imaging, its origins are not understood and only a few studies concerned with speckle reduction in OCT. Most models of OCT wash away speckle by averaging the spatial properties of the tissues in the computation of the interference signal. But this kind of averaging is not possible in practice because static tissue produces a stationary speckle pattern. There is a close connection between speckle generation and the optical band-pass response of OCT imaging systems, which makes the signal-carrying and signal-degrading roles of speckle hard to distinguish [11].

Even there are some ways of reducing the deleterious effects of speckle on OCT imaging, the noise cannot be removed totally. That is why we have to do some process on OCT images to make them clear.

3.2.4c Conclusion

(1). OCT images have much higher resolution than MRI and other machines. That is because it is based on light, rather than sound or radio frequency. Because of its high resolution it is very significant for medical science applications where scale signs are small.

(2). OCT is based on interferometry. The two beams can show structure information of the tissues and after calculation, the signals (data) go into frame grabbers(A/D converter) and then go to computers to generate images.

(3). The significant benefits of OCT are: Live sub-surface images at near-microscopic resolution; Instant, direct imaging of tissue morphology; No preparation of the sample or subject; No ionizing radiation.

(4). There are two important kinds of OCT are: TD-OCT and FD-OCT. FD-OCT has higher resolution, fast scanning speed and higher sensitivity than TD-OCT. The images we used are scanned by FD-OCT.

(5). OCT images have coherent noise which cannot be removed totally. We have to do more research on processing the images. That is kind of reason why I need to do my research to enhance the images which are not perfect.

3.3 Comments on Each Algorithm

In this section, we will write a few comments about the definition, basic background and the application of each algorithm (method).

3.3.1 The Wavelet Algorithm

This method is based on the wavelet decomposition, where the goals are to change the coefficients of each separated part in order to smooth the images. This is a frequency domain enhancement method.

A wavelet algorithm is built on the Haar wavelet, because it is the simplest one in the wavelet family. Since the original image is mostly composed by low frequencies, the wavelet method makes the image smoother by removing a majority of the high frequencies.

In this method, we change the image from RGB color space to HSV color space (defined in section 3.1). Since the Value component in HSV color space contains more information than the other parts (Saturation and Hue), we believe that the use of this part to do wavelet decomposition process is very effective. Then use Hue in HSV color space to do wavelet decomposition. After that we get four coefficients: c_A , c_H , c_V and c_D .

When we analyze this original image, we can find that the horizontal lines are the most important information. Based on this we set c_V and c_D to be zero in order to enhance the horizontal information. Filtering the c_A part using Gaussian filter (high pass filter) can give us sharper image. We do this step twice to enhance the effect. Since

wavelet decomposition will make the image a little smoother, some of the imperfect parts in the image (some parts seem lose some colors) will be filled and looks clearer.

Wavelet is commonly used in coding in image compression. But here the researcher used it to enhance the image. Wavelet transform and wavelet decomposition can separate important frequency parts of one image and by changing the coefficients of those parts, we can implement different enhancement effects. However, we believe this method could be modified since the Value component in HSV color space may not be the most effective information. We will discuss about this in Chapter 5.

3.3.2 Sobel Algorithm

In order to use Sobel operator to filter the image, we have to create a blurring low pass filter to combine with the Sobel operator and make a band pass filter. After that, the image will contain mainly the structure information and will have lost other color information as well as noise. In order to have more efficient result, the researcher timed the Sobel filter by two (see MATLAB code in Appendix) and enhanced the results.

Sobel filters are used very often in image enhancement. They are efficient and have mathematical realizations. The researcher used the most frequencies used expression, the default kind in Matlab. We may change the Blurring filter to any kind of low pass filter, which can smooth the image, but we believe this Sobel Algorithm that the

researcher used is very effective. We have changed the color information very much in this algorithm but have clearer structure information.

3.3.3 Contrast Adjustment Algorithm

In this Contrast adjustment Algorithm, I believe we have to maintain the color information to some degree; I changed the RGB image to YCbCr color space. Y component contains luminance information and the other two components, Cb and Cr store the color information. Researcher considered if we adjust the contrast in Y component and keep Cb and Cr, we will remain the color information in some extent. Contrast adjustment is very useful in gray scale images. However, since the original image is RGB image, it will bring us more problems to do enhancement. We may not keep the colors very perfect.

In the next chapter, we will present results from applying the above algorithms to OCT images of different patients. These results are further analyzed using some information theory methods.

CHAPTER 4

RESULT OF IMAGE PROCESSING AND INFORMATION THEORY ANALYSIS

4.1 Original Glaucoma Images Used in this Research

The researcher used 6 images which belonged to two patients at different times. The OCT images of these patients are shown in Figures 4.1-4.9. These images were mapped into numerical values representing the range of intensities and vectors where generated on which the information theoretic techniques were applied.

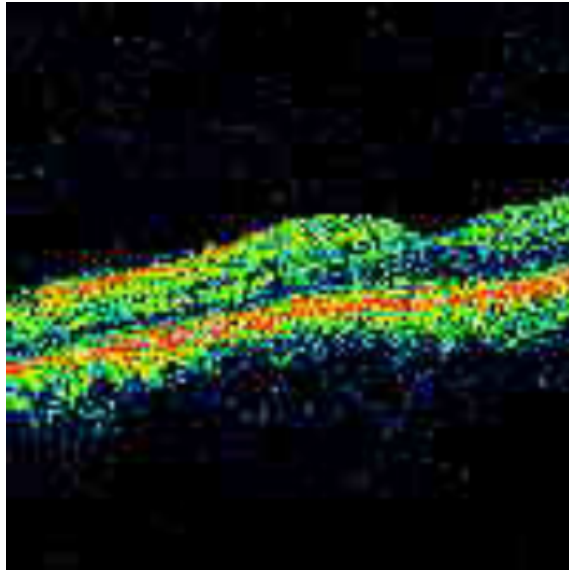
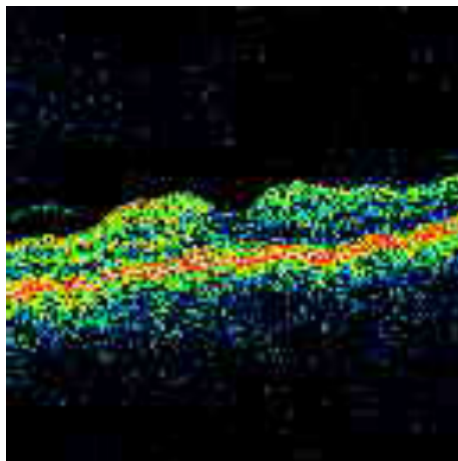
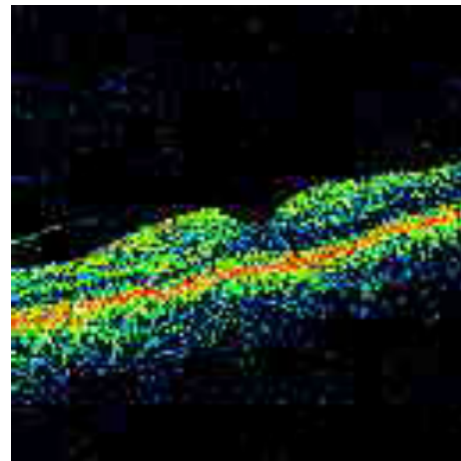


Figure 4.1 Glaucoma image of Patient A in 2005

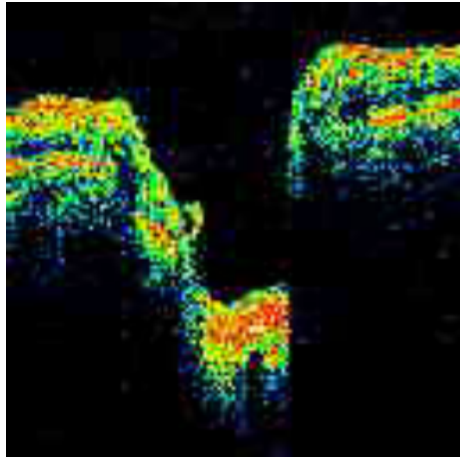


(a)

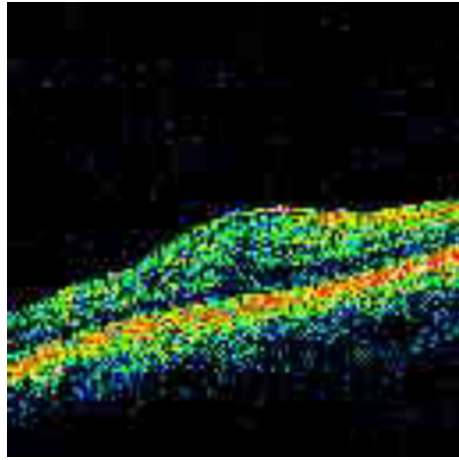


(b)

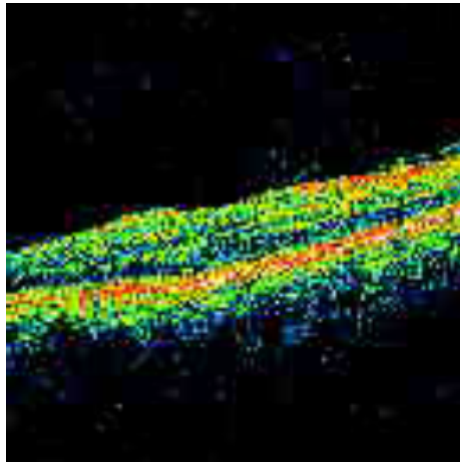
Figure 4.2 (a) Glaucoma image of Patient A in 2007 (b) Glaucoma image of patient A in 2008



(a)



(b)



(c)

Figure 4.3 (a) Glaucoma image of Patient B in 2005 (b) Glaucoma image of patient B in 04/11/2007 (c) Glaucoma image of patient B in 04/18/2007

4.2 Resulting images of the Three Algorithms

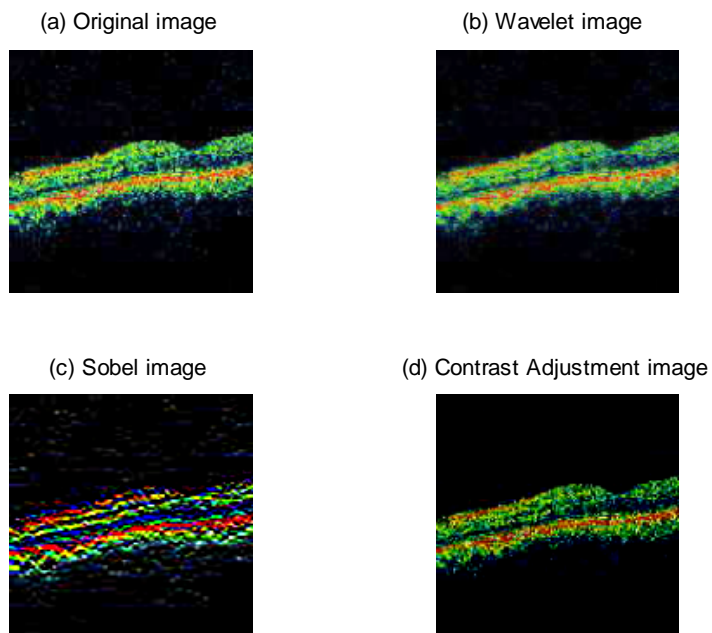


Figure 4.4 (a) (b) (c) (d) Original image, Wavelet result, Sobel result and Contrast adjustment result of Patient A in 2005, respectively

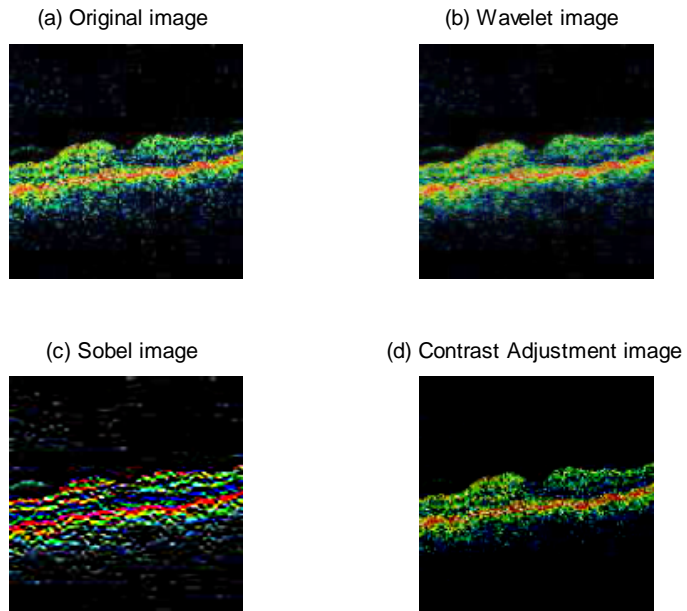


Figure 4.5 (a) (b) (c) (d) Original image, Wavelet result, Sobel result and Contrast adjustment result of Patient A in 2007, respectively

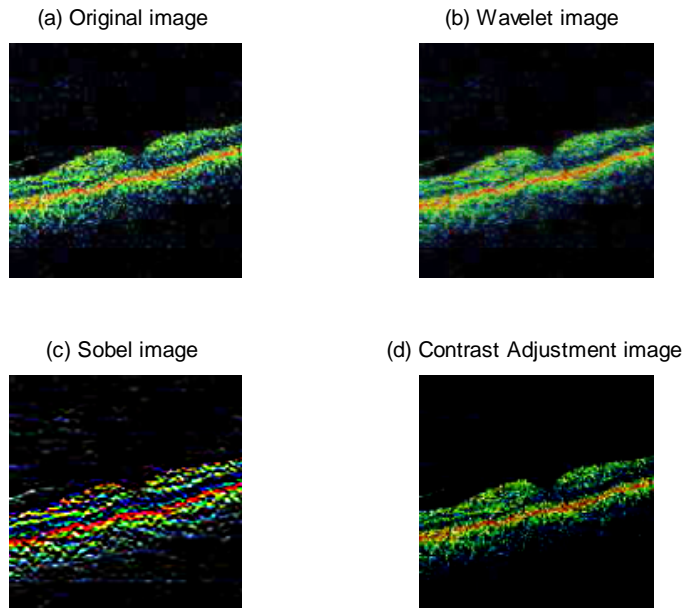


Figure 4.6 (a) (b) (c) (d) Original image, Wavelet result, Sobel result and Contrast adjustment result of Patient A in 2008, respectively

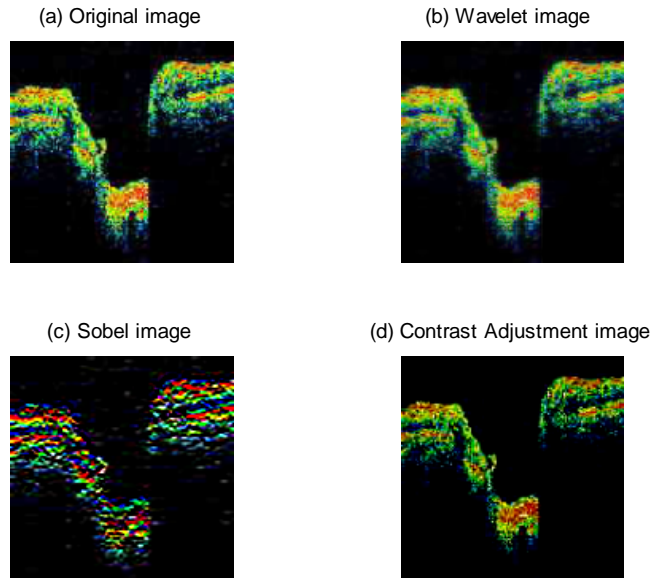


Figure 4.7 (a) (b) (c) (d) Original image, Wavelet result, Sobel result and Contrast adjustment result of Patient B in 2005, respectively

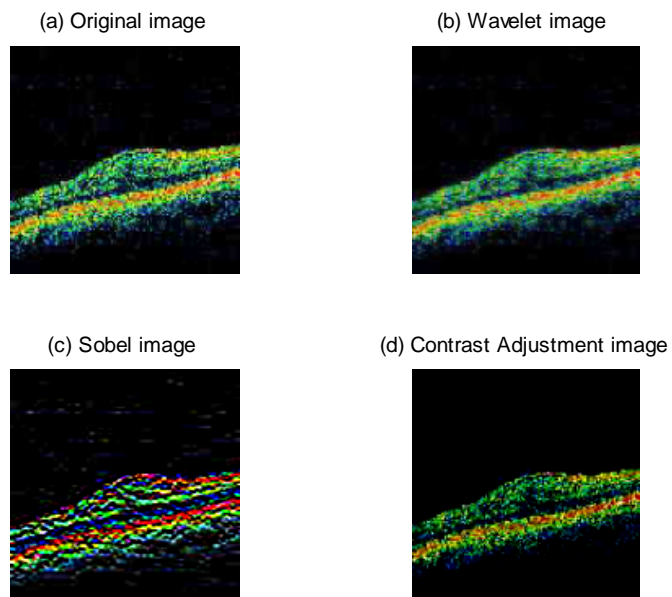


Figure 4.8 (a) (b) (c) (d) Original image, Wavelet result, Sobel result and Contrast adjustment result of Patient B in 04/11/2007, respectively

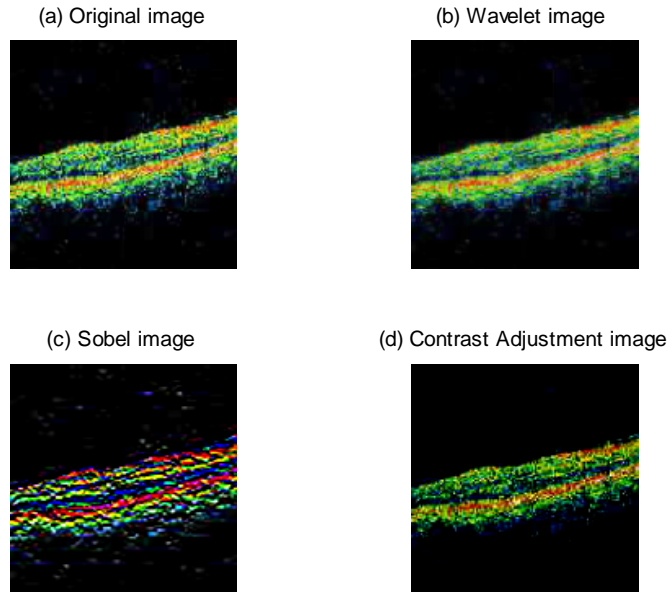


Figure 4.9 (a) (b) (c) (d) Original image, Wavelet result, Sobel result and Contrast adjustment result of Patient B in 04/17/2007, respectively

4.3 Information Theory Results

The results in this section are presented in several tables, each patient's image data in different times are presented in three tables: Table 1 to Table 6. The original images and processed images are listed on the horizontal lines and the information theory methods are listed on the vertical lines. Table 7 and Table 8 present the inner comparison of each patient's data in different years. We will discuss all of the data in Chapter 5.

4.3.1 Information Theory Data in Patient A

Table 1. Summarized Information Theory Results for Patient A in 2005

	Original Image	Wavelet Image	Sobel Image	Contrast Adjustment Image
Total Entropy	5.0029	5.1786	3.3787	1.9590
Maximum Entropy of Each Row in Image	7.7657	7.6585	6.1361	6.4464
Minimum Entropy of Each Row in Image	0.0749	0.0948	0	0
Relative Entropy From Original Image to Processed Images Method 1	0	-2799.1	-10538	-12308
Method 2	0	-0.0627	-0.3344	-0.3966
Method 3	0	-0.0627	-0.3344	1.0554
Relative Entropy From Processed Images to Original Image Method 1	0	4750	28748	38619
Method 2	0	0.0729	0.7515	1.0358
Method 3	0	0.0729	0.7515	0.8071
Mutual information(Area)		34970	17260	25431

Table 2. Summarized Information Theory Results for Patient A in 2007

	Original Image	Wavelet Image	Sobel Image	Contrast Adjustment Image
Total Entropy	5.1158	5.2724	3.4647	1.9642
Maximum Entropy of Each Row in Image	7.7892	7.6308	5.6681	6.4752
Minimum Entropy of Each Row in Image	0.6310	0.8575	0	0
Relative Entropy From Original Image to Processed Images Method 1	0	-2131.7	-9823	-11656
Method 2	0	-0.0489	-0.3270	-0.3932
Method 3	0	-0.0489	-0.3270	0.8739
Relative Entropy From Processed Images to Original Image Method 1	0	4079.4	26921	36895
Method 2	0	0.0551	0.7207	1.0174
Method 3	0	0.0551	0.7207	0.7221
Mutual information(Area)		35940	18193	25129

Table 3. Summarized Information Theory Results for Patient A in 2008

	Original Image	Wavelet Image	Sobel Image	Contrast Adjustment Image
Total Entropy	4.9755	5.1646	3.3714	1.9222
Maximum Entropy of Each Row in Image	7.6487	7.5211	5.9877	5.8153
Minimum Entropy of Each Row in Image	1.0866	1.2130	0.0953	0
Relative Entropy From Original Image to Processed Images Method 1	0	-2260.8	-10558	-12258
Method 2	0	-0.0436	-0.3338	-0.3932
Method 3	0	-0.0436	-0.3338	0.8497
Relative Entropy From Processed Images to Original Image Method 1	0	4375.6	28614	37494
Method 2	0	0.0482	0.7148	0.9645
Method 3	0	0.0482	0.7148	0.6822
Mutual information(Area)		36240	18031	24208

4.3.2 Information theory data in Patient B

Table 4. Summarized Information Theory Results for Patient B in 2005

	Original Image	Wavelet Image	Sobel Image	Contrast Adjustment Image
Total Entropy	4.7746	4.9684	3.1780	2.0844
Maximum Entropy of Each Row in Image	7.0392	6.9281	5.7507	4.8462
Minimum Entropy of Each Row in Image	0.8644	0.9281	0.4327	0
Relative Entropy From Original Image to Processed Images Method 1	0	-1817.6	-12042	-13556
Method 2	0	-0.0299	-0.3190	-0.3618
Method 3	0	-0.0299	-0.3190	0.6132
Relative Entropy From Processed Images to Original Image Method 1	0	4370.5	27747	33318
Method 2	0	0.0316	0.5808	0.7139
Method 3	0	0.0316	0.5808	0.4740
Mutual information(Area)		37213	18862	26328

Table 5. Summarized Information Theory Results for Patient B in 04/11/2007

	Original Image	Wavelet Image	Sobel Image	Contrast Adjustment Image
Total Entropy	4.7740	4.9957	3.1920	2.0371
Maximum Entropy of Each Row in Image	7.6153	7.4903	6.3255	5.6209
Minimum Entropy of Each Row in Image	0.6051	0.7162	0	0
Relative Entropy From Original Image to Processed Images Method 1	0	-637.5	-11745	-13359
Method 2	0	-0.0021	-0.3064	-0.3507
Method 3	0	-0.0021	-0.3064	0.5694
Relative Entropy From Processed Images to Original Image Method 1	0	3000.1	25406	30635
Method 2	0	0.0021	0.5204	0.6479
Method 3	0	0.0021	0.5240	0.4171
Mutual information(Area)		76333	18779	26841

Table 6. Summarized Information Theory Results for Patient B in 04/17/2007

	Original Image	Wavelet Image	Sobel Image	Contrast Adjustment Image
Total Entropy	4.6359	4.8308	3.0898	2.1384
Maximum Entropy of Each Row in Image	7.7182	7.5496	6.3584	6.1715
Minimum Entropy of Each Row in Image	0.3027	0.3506	0	0
Relative Entropy From Original Image to Processed Images Method 1	0	-2043.7	-12874	-14215
Method 2	0	-0.0304	-0.3011	-0.3347
Method 3	0	-0.0304	-0.3011	0.5678
Relative Entropy From Processed Images to Original Image Method 1	0	5649.1	28206	32355
Method 2	0	0.0319	0.4963	0.5832
Method 3	0	0.0319	0.4963	0.3945
Mutual information(Area)		37458	18732	28242

4.3.2 Inner Comparison of Sequential Images in Patient A and B

In Table 7 and Table 8, we list all of the information theory results between the sequential images of Patient A and Patient B, respectively. In the tables, Method 1-Method 5 were introduced in Chapter 3. We will discuss the results in Chapter 5.

Table 7 Inner Comparison of Sequential Images of Patient A

	Original Image	Wavelet Image	Sobel Image	Contrast Adjustment Image
Relative entropy 05-07 Method 1	288.2	214.1	300.6	90.3
Method 2	-0.0099	0.0123	0.0173	0.0052
Method 3	0.0238	-0.0002	-0.0004	-0.0099
Relative entropy 07-05 Method 1	770.6	-208.7	-295.0	-89.9
Method 2	0.0101	-0.0120	-0.0169	-0.0052
Method 3	0.0240	0.0002	0.0004	0.0097
Mutual information of 05-07 Method 4	51340	79522	17333	96744
Method 5	68559	79567	65515	98525
Relative entropy 05-08 Method 1	-50.3	-76.7	-186.2	29.2
Method 2	-0.0302	-0.0045	-0.0108	0.0017
Method 3	0.0165	0.00003	0.00018	0.0111
Relative entropy 08-05 Method 1	929.1	77.4	188.4	-29.2
Method 2	0.0324	0.0045	0.0109	-0.0017
Method 3	0.0168	0.00003	0.00018	0.0107
Mutual information of 05-08 Method 4	31607	76543	66044	91328
Method 5	66021	79076	66104	95703
Relative entropy 07-08 Method 1	551.9	-294.5	-534.0	-66.8
Method 2	-0.0209	-0.0154	-0.0279	-0.0035
Method 3	0.0092	0.0004	0.0012	0.0042
Relative entropy 08-07 Method 1	573.2	304.4	550.6	67.0
Method 2	0.0220	0.0159	0.0288	0.0035
Method 3	0.0090	0.0004	0.0012	0.0040
Mutual information of 07-08 Method 4	34140	59305	16473	91149
Method 5	70635	82143	65135	95004

Table 8 Inner Comparison of Sequential Images of Patient B

	Original Image	Wavelet Image	Sobel Image	Contrast Adjustment Image
Relative entropy 05-07a Method 1	268.1	-118.6	-87.7	-57.3
Method 2	-0.0375	-0.0101	-0.0075	-0.0049
Method 3	0.0166	0.00015	0.00009	0.0118
Relative entropy 07a-05 Method 1	1528.1	120.8	88.4	57.6
Method 2	0.0402	0.0103	0.0075	0.0049
Method 3	0.0162	0.00015	0.00009	0.0101
Mutual information of 05-07a Method 4	11386	49905	58123	59171
Method 5	64518	72106	66019	82164
Relative entropy 05-07b Method 1	-243.5	-1229.7	-455.2	6.2067
Method 2	-0.0657	-0.0634	-0.0235	0.0003
Method 3	0.0181	0.0064	0.0009	0.0080
Relative entropy 07b-05 Method 1	2663.8	1374.8	466.4	-6.2048
Method 2	0.0742	0.0709	0.0240	-0.0003
Method 3	0.0177	0.0064	0.0009	0.0078
Mutual information of 05-07b Method 4	15568	40196	11325	61289
Method 5	66336	75198	66671	84799
Relative entropy 07a-07bMethod1	943.8	-13547	-440.0	130.3
Method 2	-0.0304	-0.0540	-0.0176	0.0052
Method 3	0.0166	0.0045	0.0005	0.0099
Relative entropy 07a-07bMethod1	2209.5	1487.3	448.0	-129.6
Method 2	0.0321	0.0593	0.0179	-0.0052
Method 3	0.0166	0.0046	0.0005	0.0110
Mutual information of 07a-07bMethod4	29900	46143	13375	85443
Method 5	73254	78513	69403	97836

4.4 Results of Correlation

In order to know the relationships of the six images shown below, the similarities (for example, from the same patient), correlations, using Excel, were calculated.

Table 9. Correlation of Patient A Images in Different Periods

Patient A	06/14/2005 (a)	06/12/2007 (b)	05/29/2008 (c)
06/14/2005 (a)	1.0000		
06/12/2007 (b)	0.9944	1.0000	
05/29/2008 (c)	0.9967	0.9990	1.0000

Table 10. Correlation of Patient B Images in Different Periods

Patient B	03/09/2005 (a)	04/11/2007 (b)	04/18/2007 (c)
03/09/2005 (a)	1.0000		
04/11/2007 (b)	0.9973	1.0000	
04/18/2007 (c)	0.9971	0.9994	1.0000

Table 11. Correlation of Patient A Images in Different Enhancement Methods

Patient A	Original image	Wavelet image	Sobel image	Contrast Adjustment image
Original image	1			
Wavelet image	0.9789	1		
	0.9856			
	0.9804			
Sobel image	0.8954	0.7860	1	
	0.9287	0.8544		
	0.9267	0.8357		
Contrast Adjustment image	0.8769	0.7612	0.9983	1
	0.9152	0.8368	0.9988	
	0.9126	0.8160	0.9988	

Table 12. Correlation of Patient B Images in Different Enhancement Methods

Patient B	Original image	Wavelet image	Sobel image	Contrast Adjustment image
Original image	1			
Wavelet image	0.9923	1		
	0.9845			
	0.9939			
Sobel image	0.9695	0.9325	1	
	0.9812	0.9341		
	0.9823	0.9563		
Contrast Adjustment image	0.9606	0.9201	0.9990	1
	0.9755	0.9248	0.9993	
	0.9755	0.9463	0.9990	

In the results of relative entropy of Original image and Contrast Adjustment image in Method 3, we also get different values from Method 1 and Method 2 (column 4). In order to find out the trend based on Gamma (equation 8 in Chapter 3), I calculated Table 13.

Table 13. Different Gamma Values of Patient A in 2005

Gamma	0.4	0.8	1.2	1.4	1.8
Relative Entropy from the Original image to Contrast Adjustment Image(Method 1)	-11078	-11575	-12017	-12137	-12308
Method 2	-0.3534	-0.3709	-0.3864	-0.3906	-0.3966
Method 3	1.9568	1.1646	1.0864	1.0727	1.0554
Relative Entropy from the Contrast Adjustment image to Original image	31530	34265	36841	37568	38619
Method 2	0.8314	0.9102	0.9845	1.0055	1.0358
Method 3	1.4029	0.8238	0.7831	0.7884	0.8071
Mutual information of Original image and Contrast Adjustment image	34635	31420	27604	26691	25431

4.4 Histograms

Figure 4.10-4.17 show histograms of OCT images for Patient A and Patient B. The tables of the plots asymptotically approaches zero around an intensity of 200. In order to make the curves clear enough, we only plot part of the curves (intensities from 0 to 40, frequency numbers from 0 to 6000).

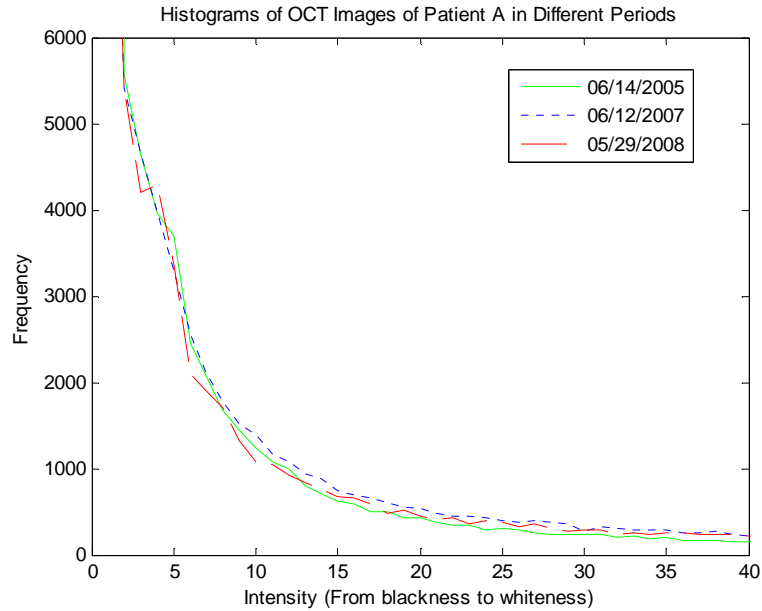


Figure 4.10 Histograms of Sequential OCT Images of Patient A

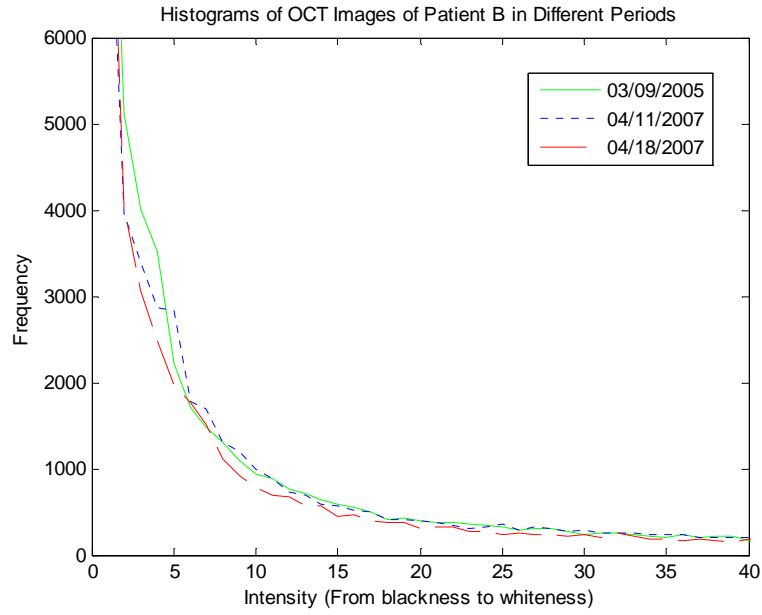


Figure 4.11 Histograms of Sequential OCT Images of Patient B

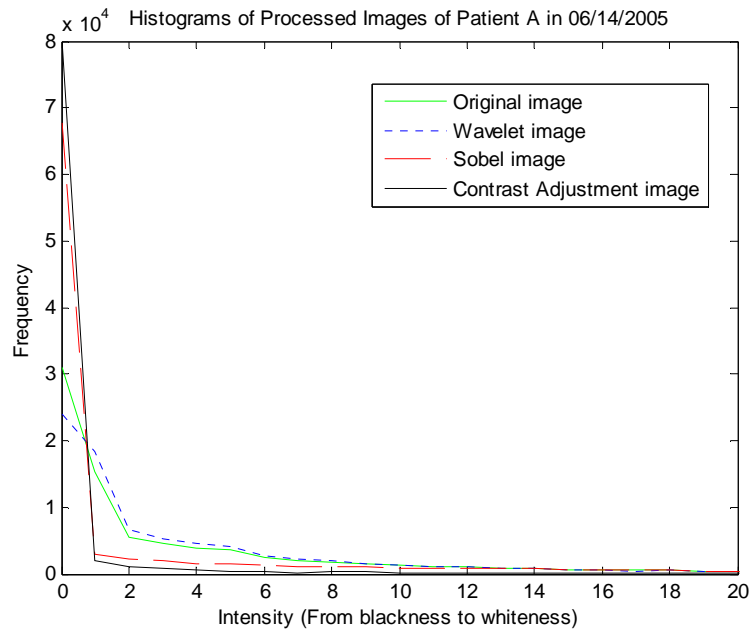


Figure 4.12 Histograms of OCT Images of Patient A in 2005

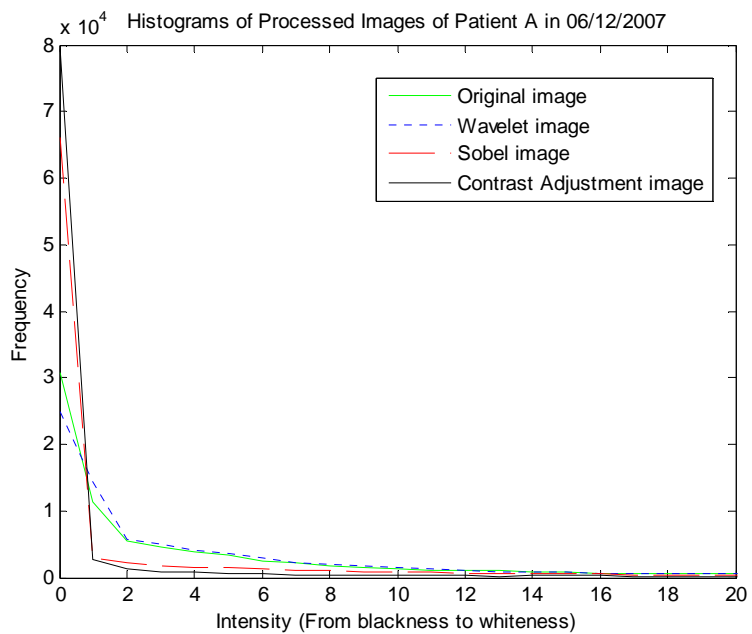


Figure 4.13 Histograms of OCT Images of Patient A in 2007

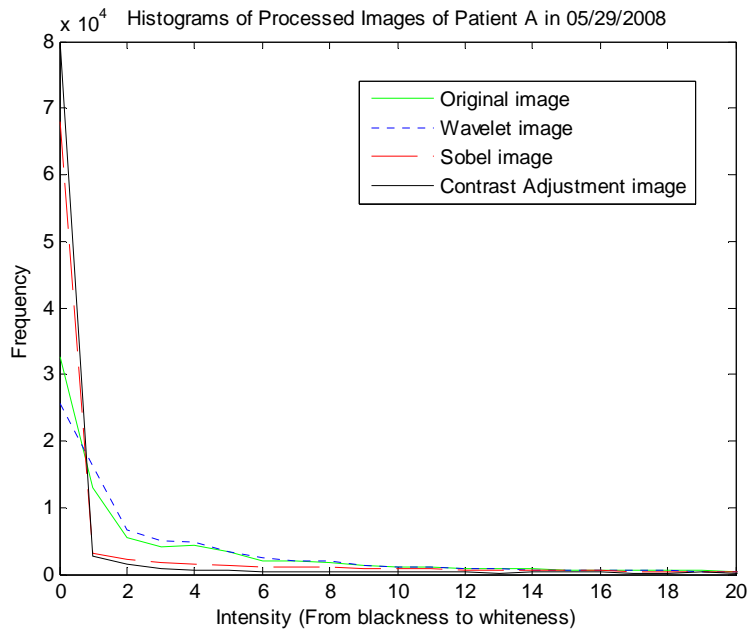


Figure 4.14 Histograms of OCT Images of Patient A in 2008

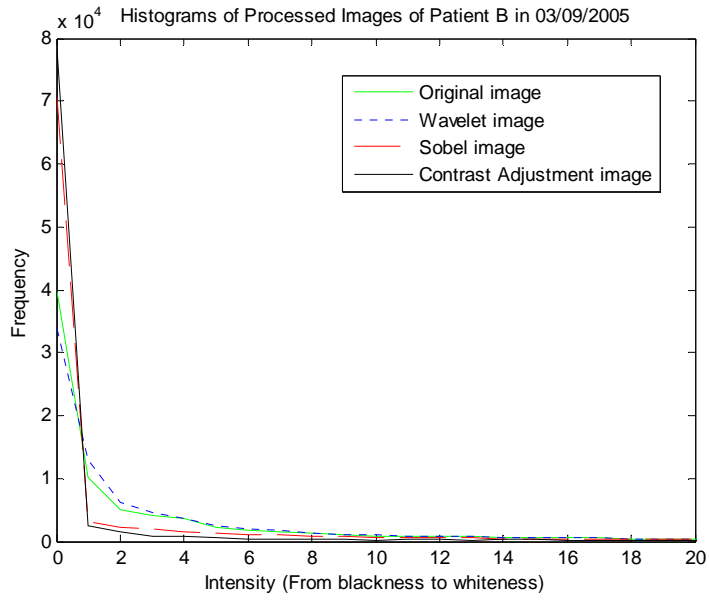


Figure 4.15 Histograms of OCT Images of Patient B in 2005

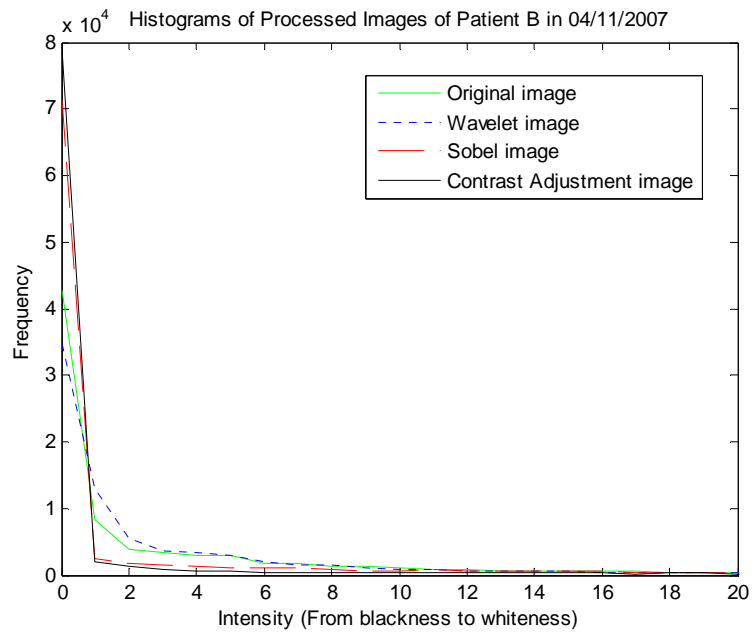


Figure 4.16 Histograms of OCT Images of Patient B in 04/11/2007

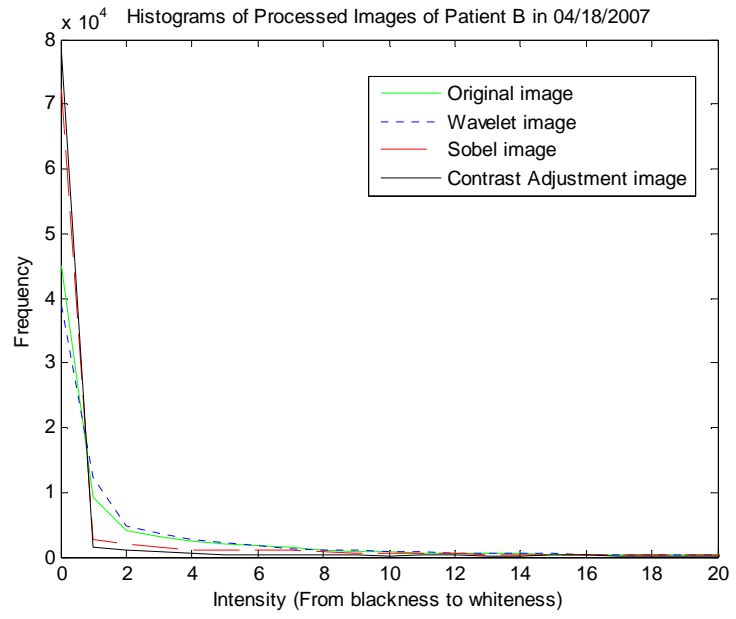


Figure 4.17 Histograms of OCT Images of Patient B in 04/18/2005

CHAPTER 5

DISCUSSIONS AND FUTURE RESEARCH

In this Chapter, we will have discussions about the result images and tables in Chapter 4. Firstly, we will analyze and compare the results of the three image enhancement algorithms; secondly, we will compare and find out the relationships (trends) of the information theory results; finally, we will discuss which method is the best method for glaucoma images scanned by OCT, in other words, which method can give us more information.

All of the comparison and analysis of information theory are classified into two ways: comparison of different enhancement algorithm and comparison of different periods of the same patient.

5.1 Comparative Analysis of Algorithms

In this section, we will compare the results of the three enhancement algorithms and make some comments. These comments will be made with reference to the models in Chapter 3 and the results in Chapter 4.

5.1.1 Results of Wavelet Algorithm

In the glaucoma images, different colors represent different tissues in the human eye. As shown in image (b) in Figure 4.4-4.9 in Section 4.1, the wavelet images are slightly blurred compared to original images, some parts of the lines are clear. As we can see in the original images, structures are not totally filled with colors; there are some “holes” (uncolored small areas) in them. After applying wavelet algorithm, the “holes” are filled and the structures and tissues are clearer and visible. We consume that we added some information to the images by applying wavelet algorithm. Sequential images of the patient’s eye will be needed to validate the accuracy of the added structures, as we see from Chapter 3 and Chapter 4.

5.1.2 Results of Sobel Algorithm

The original image has several horizontal lines that are kind of indistinguishable from each other. The resulting images (Figure 4.4-4.9) show the distinct horizontal lines are clearer than the lines in original images. In other words, after using the Sobel operator we can see the horizontal lines clearly in the resulting images. Most tissues (cells) between the horizontal lines are removed, leaving the horizontal lines in the images. This Sobel algorithm is very useful to extract the structures in the images, we believe doctors can find out the distances between different tissues in the glaucoma images easier. The

only problem is, this algorithm changes the colors of the lines and we need to figure out the corresponding lines from the original images.

“Ophthalmologists would like programs that highlight different layers of the retina and where pathologies are, such as the way your Sobel image did, but the layers should be different colors”. This is from Dr Mayer, assistant clinical professor at Yale School of Medicine. We believe that the Sobel Algorithm is very meaningful in this case (refer to Chapter 2).

5.1.3 Results of Contrast Adjustment Algorithm

Researcher chose gamma (see equation 3.8 in Chapter 3) to be 1.8 and have the resulting images. The contrast was adjusted and colors were darker than original images. As we can see from the resulting images in Figure 4.4-4.9 image (d), some parts of the structural lines are clearer because of the higher contrast with the gamma value.

However, we can find from the results that this method also makes the image lose some useful information, which cannot be avoided. For example, the left part and right part of the horizontal lines are of lower intensities, while the center part is advanced and is clearly shown. The problem is that we cannot remove the background noise and the useless information completely. However, without removing useful information, there is still some noise left in the images.

Generally speaking, the image enhancement methods used in this paper can also be used in gray scale images. However, since in OCT scanned Glaucoma images, colors are very significant in identifying the cellular structures. Different color represents different structures and tissues. Hence, we should think about colors when we create the enhancement algorithms.

5.2 Analysis of Information Theory

In this section, we will analyze and compare the results of entropy, relative entropy and mutual information analyzes of the processed image results. All of the discussions and comparison are based on Table 1 to Table 8 in Chapter 4.

5.2.1 Entropy Results

In Table 1 to Table 8 of Chapter 4, the total entropy is calculated using Matlab function, and normalized probabilities of histograms.

a. Comparison of different enhancement algorithms

In Table 1 to Table 6, the data of total entropy of the wavelet results (row 1, column 2) are slightly larger than the results of original images (row 1, column 1), respectively. The total entropy values of the Sobel results (row 1, column 3) are smaller than the results of original ones, and contrast adjustment results (row 1, column 4) are the smallest.

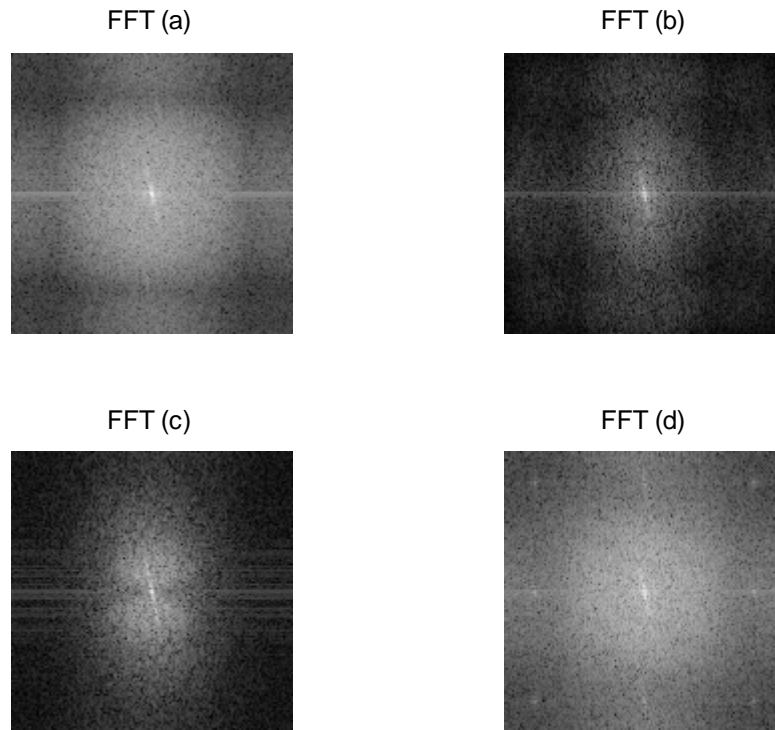


Figure 5.1 FFT (Fast Fourier Transform) of the OCT image of Patient B in 2005, (a) (b) (c) (d) correspond to original image, wavelet image, Sobel image and Contrast adjustment image, respectively

It means the Sobel algorithm and the contrast adjustment method remove more noises from the original images than the wavelet algorithm. Hence, the uncertainties of the processed images are reduced as shown in the total entropy results, especially the Sobel image and the contrast adjustment image. That is because Sobel image used a band pass filter (Sobel operator and blurring filter), which filtered a lot of the high frequencies and the low frequencies from the image as was introduced in Chapter 3. The FFT of Sobel images (Figure 5.1) show the frequencies are becoming larger variance. It removed

some of the high frequencies and maintained the significant high frequencies which correspond to the structural information, which suggest the edges are clearer than before and noise are removed. The main low frequencies are maintained and most of the medium frequencies are reduced which suggests we already removed some useless information (not the structural information) and enhance the structural lines. The Sobel images are very successful to show the significant structures (refer to Dr. Mayer's words in Chapter 2).

Because the colors of the images are darker by the parameter gamma set to 1.8 as mentioned in Chapter 3, the adjustment of contrast change the intensities of an image to make them balanced. The FFT of the images show more uniform spectrum than the FFT of original images. The method of contrast adjustment is similar to a band pass filter, so some high and low frequencies are removed by this method. The spectrum is more spectrally balanced, meaning we added more high frequencies. The contrast adjustment images are also successful to show the structures clearer than before.

For wavelet images, the total entropy is slightly increased than original images. From the FFT spectrum, we can see that it still maintain the low frequencies of the original images, and it removed some high frequencies, which we believe is noise. It also added some high frequencies to the images. This is why the total entropy is increased. These high frequencies made the structural lines of the wavelet images clearer than before. We can see clearly that the low frequencies are enhanced visually by removing some of the high frequencies and some medium frequencies.

As was mentioned before, we can find that there are some “holes”(uncolored small areas) in the structures between the horizontal lines in the original images. The wavelet images are slightly blurred and some of the “holes” are filled, which means we added some information to the images. Here wavelet has made the images slightly smooth (less fine structures), as a result, there is a slightly increase in the entropy of the images (see the results in Table 1 though Table 6, row 1). For example, in Table 1 for Patient A, the total entropy of the wavelet image is 5.1786 and is 5.0029 for original image.

We did not compare the total entropy of images of the same patient because the mutual information, the relative entropy and the correlation coefficients were sufficient to show these relationships.

5.2.2 Relative Entropy Results

Relative entropy shows that which two images are more similar or more related in their distributions of intensity histograms. The smaller the value, the more similar the distributions of the histograms of the images are. We can see from table 7 (Patient A), from the original images, the image in 2008 is more related to the image in 2005. From the mutual information, the image in 2005 and 2007 are more similar.

This suggests the structures and distributions of the three images are very similar. The health level of Patient A is very stable.

a. Comparison of different enhancement algorithms

In Tables 1-6, we present two results: relative entropy values for the original image versus the three processed images (row 4, 5 and 6 in Table 1 to Table 6) and the relative entropy values from the three processed images versus the original image (row 7, 8 and 9 in Table 1 to Table 6). Since we know if the elements of the matrix of probabilities p is greater than the elements of matrix of probabilities q , relative entropy is positive (see equation 3.10). Therefore, the elements of wavelet matrix of probabilities, the elements of Sobel matrix of probabilities and the elements of the Contrast adjustment matrix of probabilities are greater than the original elements of matrix of probabilities. Herein, the matrix of probabilities is generated by probabilities of pixels appeared in the image (see section 4.2).

The matrix of probabilities is different from the normal probability mass function we used in information theory. When we remove some of the noise from the original images, the resulting images are more “ordered”, which means the information is stable. For Sobel results and contrast adjustment results, the distributions of intensities have a larger variance. For wavelet results, the distributions of intensities are more equalized (Figure 4.12-4.17). The larger variance histograms will make the matrix of probabilities of the result images larger than the matrix of probabilities in original images (see equation 3.10 in Chapter 3). The equalized histograms will increase the probability

vectors which are generated by normalized histograms. Since the conditions in Method 2 and Method 3 (see Chapter 3) were used, we get the calculation with nonzero probability vectors and nonzero matrix of probabilities. All of those reasons lead to the increase of the probability vectors and matrix of probabilities.

b. Comparison of sequential images of the same patient.

In Table 7, relative entropy results for images from 2005 versus 2007 (row 1, 2 and 3, column 1) are larger than results from 2007 versus 2005 (row 4, 5 and 6, column 1) in Method 1 and Method 2 (see Chapter 3). This means that the elements of the matrix of probabilities and probability matrix of Patient A in 2007 is larger than the matrix of probabilities and probability matrix of Patient A in 2005 of original images. This suggests the distribution of the original image is not the same and the intensity distribution of the processed images. We consider that the background (almost black) areas are larger in image taken in 2007 than the background areas in 2005. Some unhealthy structures are removed or some healthy structures are destroyed. It helped to analyze the areas of the structures and tissues, for the comparison in sequential images taken in different period of the same patient. However, if we would like to know the accurate information, we have to acquire more data. The results are the same when we computed 2005 versus 2008 and 2008 versus 2007 and the same results in Table 8. In Method 3, the relative entropy results show different results. That is because the conditions are different (see Chapter 3). The relative entropy of the original image in Patient A in 2007 versus 2008 is slightly smaller than the relative entropy in Patient A in 2008 versus 2007. This suggests that the two intensity distributions are close in shape.

This researcher believes the matrix of probabilities contains the position information of the intensities in an image, results of Method 1 is valuable. However, in the definition of relative entropy in Chapter 3, the matrices must be probability mass function which sum to 1. The summation of the matrix of probabilities is not equal to 1, however. Therefore, Method 2 and Method 3 are appropriate here because they are calculated based on normalized histograms. Method 2 is reasonable in Table 1 though Table 6 where we have the lateral comparison of the original images and the processed images. This gives the relationships of the four different images. In Table 7 and Table 8, since we calculated the relative entropy of one year versus another year, we have set respective conditions of different pairs using Method 3. Therefore, Method 3 is more reasonable in this situation, because of the selected conditions.

5.2.3 Mutual Information Results

a. Comparison of different enhancement algorithms

For mutual information (row 10, Table 1 to Table 6), the wavelet images are more similar with the original images. That is because the wavelet images maintain most of the color information. The Sobel algorithm changed too much color information of the images, only leaving edges, so the Sobel images have more differences from the original images. However, Dr. Hylton Mayer, at Yale University Medical School, stated this was good for the doctor's work.

b. Comparison of sequential images of the same patient.

In Table 7 and Table 8, we used two ways to calculate mutual information (see Chapter 3). We believe Method 5 is more reasonable in this situation as we analyzed in Chapter 3.

As we can see, mutual information results have some differences from the relative entropy results. There are two reasons: (1) Researcher calculated mutual information based on the overlap areas from matrix of probabilities of each image, which means mutual information itself is more concentrated on areas. However, relative entropy (Method 2 and 3) is calculated based on histograms, which lose the position results as we talked before in section 5.2.2. (2) Besides, conditions of removing zeros in Method 2 and Method 3 can affect the results (see introduction in Chapter 3).

5.2.4 Gamma

In Table 13, Gamma is from a Matlab function “imadjust”: $J = \text{imadjust}(I, [\text{low_in}; \text{high_in}], [\text{low_out}; \text{high_out}], \text{gamma})$ (equation 3.8 in Chapter 3). Gamma specifies the shape of the curve describing the relationship between the values in I and J. If gamma is less than 1, the mapping is weighted toward higher (brighter) output values. If gamma is greater than 1, the mapping is weighted toward lower (darker) output values. If one omits the argument, gamma defaults to 1 (linear mapping) [5].

Here we used 5 different gamma values in order to find out the trends of the information theory results based on gamma. Table 13 shows all of the results. We can see as the increase of the gamma values, the absolute values of the relative entropy from the original image to the contrast adjustment image (Method 1) and the relative entropy from the contrast adjustment image to original image are increasing. It means when the gamma values are increasing, the differences between the two images are increasing. It has the same trend in method 2.

In results of Method 3, the relative entropy of the original image to contrast adjustment image is decreasing, while the relative entropy results from the contrast adjustment image to original image has a different trend. Results of Method 3 suggest the two images are getting more similar to each other, which is opposite with the trend of Method 1 and Method 2. In my opinion, this way of calculating the relative entropy is not very perfect. All of the pairs should be calculated based on the same condition (the same as Method 2. Matlab Code in Appendix). The results are different with Method 1 and Method 2.

The researcher also calculated the mutual information in Table 13. It is decreasing which corresponds to the increase of the relative entropy. In this situation, if the mutual information result is large, it means the two images are very similar. The decrease of the mutual information and increase of the relative entropy tell us, as the gamma value is growing up, the two images are more and more different in intensity histograms and in matrix of probabilities.

5.2.5 Correlation Results

a. Comparison of different enhancement algorithms

In Table 11 and 12, different rows of each correlation pairs are based on different enhancement algorithms. Generally speaking, the most correlated pairs are: the original image and wavelet image, Sobel image and contrast adjustment image. Wavelet image maintains more information from the original images. Sobel images and contrast adjustment images are more similar, which is the same conclusion as we analyzed in the total entropy results in section 5.2.1.

b. Comparison of sequential images of the same patient.

From Table 9 and Table 10, the values are large enough to say that they are very correlated. It means, they all remain the useful information or they have some information that is the same. In other words, they are from the same patient. The most correlated pairs are, 2007 to 2008 in Patient A (Table 9), which have the correlation coefficient 0.9990 and 04/11/2007 to 04/18/2007 in Patient B, which have the correlation coefficient 0.9994 (Table 10). We consider that the health level of Patient A between 2007 and 2008 is similar and stable, and Patient B was becoming much healthier in 2007 than 2005, and after one week, Patient B was continuing recovering. Since time is very limit, the healthy level did not change too much.

However, there are problems in this kind of method: the artificial colors in the images cannot be the same, means the intensities of the images are different, even if the images are from the same patient, correlation values could be very small; even if the images are from the same patient, the health level can be different to give different results. So this correlation method can only give us some general ideas and general trends. Any of these problems can greatly affect the correlation results.

However, we should understand that the correlation results can only tell us which two images are more correlated. If we want to determine which two images are from the same patient, we should know more data.

We also presented histograms of images of Patient A and Patient B in different times. There are only slightly differences among different times (Figure 4.10-4.11), meaning that we cannot find out sufficient information of the trends only from the histograms.

5.3 Best Method

After the analysis in Section 5.1 and 5.2, we already know the usages of Information Theory. What we want to determine is which way is the best way of information theory in diagnosis analysis. In other words, which Information theory method will provide doctors with the most supplemental information concerning the state of the patient's glaucoma.

Entropy tells us uncertainties of the images. It cannot give us detailed information. Generally speaking, the larger the entropy is, the large uncertainty has in an image, and the more noise in the image. There is also a particular case, the wavelet image. Although wavelet can remove some frequencies from the original image, actually it adds some more information into the image. Sobel and contrast adjustment methods are band pass filters essentially.

In the three methods in calculating relative entropy, researcher believes Method 1, Method 2 and Method 3 are reasonable based on different situations (see section 5.2.2)

Mutual information is calculated based on overlap areas in the reference paper. Researcher set the tolerance value of the comparison between the two matrices of probability to be 0.01. If we decrease the tolerance value, the overlap areas of the original image and contrast adjustment image will be increased. It shows some areas of the two images are very similar but more areas of original image and wavelet image are less similar but similar enough. Researcher does not need to set the tolerance value to be too small, we believe 0.05 is enough to show the similarities in statistics.

Different image enhancement methods will bring different kind of images. The intensities of Wavelet image and Sobel image are between 0 and 1. Since I need to compare the histograms of the result images, researcher multiplied each intensity value

by 255 and floored the results. Researcher believes that is a good way to solve this range problem. But it will bring some inaccuracy.

The mutual information result is different from the relative entropy in the comparison of original image and Sobel image, Original image and contrast adjustment image. They are all correct results. The point is mutual information and relative entropy show different information in different angles as we mentioned before.

Relative entropy results of Method 3 in Table 7 tell us, the images of Patient A in 2007 and 2008 have more relationship than the images of Patient A in 2005 and 2008, then the images in 2005 and 2007 have least relationship. From the mutual information results, the images of Patient A in 2007 and 2008 have more relationship. The images in 2008 and 2005 have less relationship.

Relative entropy and mutual information results suggest the same conclusion that the most related pair is images in 2007 and 2008. However, the results of relative entropy and mutual information have conflict in the other two pairs. This researcher calculated the mutual information based on overlap areas, which means it focuses on the areas of the structures. The relative entropy and correlation are based on histograms, which lose the position information of intensities and are more concentrated on the distributions. The same result trends happened in Table 8 of Patient B.

Since the Sobel image is a structure image, it has less areas, the mutual information of Sobel image and original image is less than the original image and contrast adjustment image, which is opposite in relative entropy and correlation.

We believe that in order to find out the correct and useful information for diagnosis, we need to combine entropy, relative entropy, mutual information and correlation together. There is no perfect method to show 100% information.

5.4 Future Work

In this section, we will talk about the future work of this project. In Figure 1.2 in Chapter 1, researcher presented block diagram of the whole process of image processing. Researcher believes we still need to modify the enhancement algorithms, use edge detections to find exact edges and measure the distances between the horizontal lines.

But only enhancement is quite insufficient. After enhancement, the contrast of the image is increased, we will do edge detection in order to gain the edge lines of the structures. Then, we can measure the exact distances between (among) the different layers. The whole process is shown below:

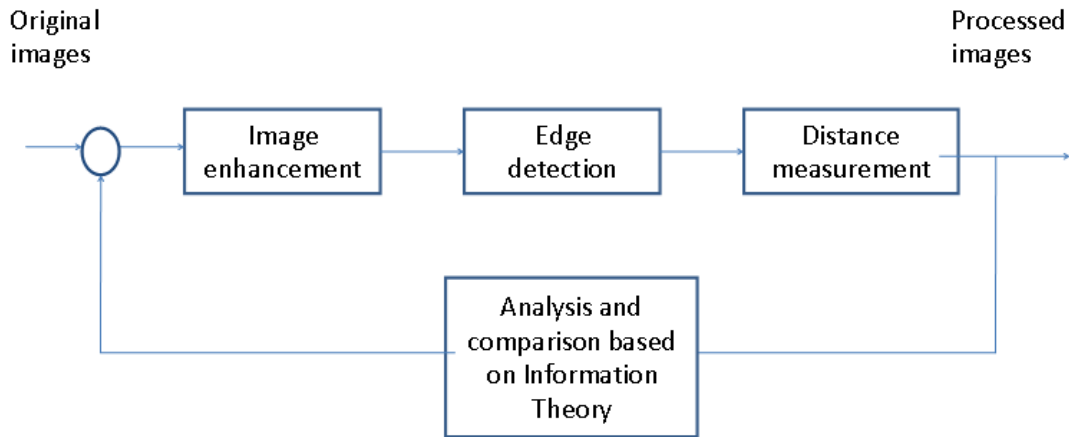


Figure 5.2 Block diagram of the process

5.4.1 Modified Wavelet Algorithm

In the wavelet algorithm introduced in Chapter 3, researcher use V part in the HSV color space, filtered by a kind of Sobel filter. In the new wavelet algorithm, we could change the V part to H part, that is, Hue. That is because in the HSV color space, H part also has a lot of information, even more than V part. The problem is, filtering H part will change the color information of the image. In the wavelet decomposition, researcher used average filter, and the Haar wavelet, which is the most basic wavelet. In order to get more precise result, we can use “dB2” (a kind of wavelet) instead of Haar wavelet.

5.4.2 Remove Blue from Glaucoma Images

From the glaucoma images, since the red lines are really important, the yellow and green parts are also important. When we separate the RGB image to “RG” image, it

did not show any difference to RGB image. It is clear that the blue, especially the points which have more blue are noise. So researcher thinks about trying to remove them.

As we can see, in some places of the image, the blue points are almost totally removed. In the middle of the image, the edges are getting clearer than before. However, the shortcoming is that, it did remove the useful information on the side of the image, which is blue and has more blue.

The future work would be: find the best threshold values to maintain the edge information; or use dynamic test to remove the different blue points.

5.4.3 Edge Detection

Based on the three processed images, we can do edge detection with “canny”, a very useful edge detection method. The most powerful edge-detection method that edge provides is the Canny method. The Canny method differs from the other edge-detection methods in that it uses two different thresholds (to detect strong and weak edges), and includes the weak edges in the output only if they are connected to strong edges. This method is therefore less likely than the others to be fooled by noise, and more likely to detect true weak edges.

5.4.4 Distance Measurement

Since the distances between the horizontal lines in the images are quite important, which will be helpful for doctors to figure out whether the tissues between the horizontal lines are complete and whether the patient is healthy, researcher needs to calculate the distances. Researcher used Matlab to realize the algorithm: choose two points randomly in the image, the algorithm will tell you the distance and the coordinates of them.

5.5 Conclusion

Glaucoma may be the second leading cause of blindness in the world, affecting about 60 million people globally. Nowadays, people use Optical Coherence Tomography (OCT) to diagnosis of glaucoma. The patients' eyes are scanned by OCT and we obtain the macular images from the back of the eyes. However, OCT images usually contain noise and it is sometimes difficult for doctors to diagnosis.

In the original images shown in Chapter 2, we know that different colors represent different structures and layers in the eye. Hence, to highlight and enhance the structures and edges in the glaucoma images are the most important thing we should do.

Therefore, image enhancement techniques can remove the noise from the images and highlight the structures of the glaucoma images. It can help doctors to better analysis of OCT images and diagnosis of glaucoma. In this thesis, we provided three successful algorithms for enhancing the quality and the contrast of OCT images. The resulting images in Chapter 4 show that our algorithms can remove noise and enhance the horizontal structures in images, significantly enhancing the visual quality of the glaucoma images.

From the results of Information theory, we believe that it is very useful to show the trends between the systems, and having more sequential images will provide more trend information. By using information theory, we obtain standard measurement of the relationships among the three algorithms. From the analysis of the information theory results we are clear about the health level of the sequential images taken in different time of a same patient. Information theory successfully helped to provide trends among the sequential images, which will help doctors to diagnosis.

References

- [1] Rafael C.Gonzalez, Richard E.Woods, Digital image processing. Second edition. Prentice Hall. 2004
- [2] Gerald Kaiser, A Friendly Guide to Wavelets. First edition. Birkhauser. 1994
- [3] Rafael C.Gonzalez, Richard E.Woods and Steven L.Eddins, Digital image processing using matlab. Second edition. Prentice Hall. 2004
- [4] Daniel M Albert, Joan W. Miller, Dimitri T. Azar, and Barbara A. Blodi, Principles and practice of ophthalmology. Alberts Jakobiec's, volume . Third edition. Saunders.2008.
- [5] Matlab help doc (version 7.1.0.246 August 02 2005).
- [6] Brett E Bouma and Guillermo J. Tearney, Eds. Handbook of Optical Coherence Tomography. New York: Marcel Dekker, 2001.
- [7] Dr. Hylton Mayer. hylton.mayer@yale.edu (06/02/2009)
- [8] John D Monnier, "Optical Interferometry in Astronomy".2003
- [9] Chien-Wen Chang, "Stuidies on Diffraction Gratings Pair Over Fourier Domain Optical Coherence Tomography". Institute of Electro-Optical Science and Engineering National Cheng Kung University. June 2008
- [10] Douglas A. Lind, William G. Marchal and Samuel A. Wathen, Statistical Techniques in Business and Economics. Thirteenth Edition. McGraw-Hill Irwin. 2008.
- [11] Joseph M. Schmitt, "Optical Coherence Tomography(OCT): A Review," IEEE J.Select. Topics Quantum Electron., vol.5, pp. 1205-1215, July-Aug 1999.
- [12] Theodor Richardson (richa268@enr.sc.edu).Improving the Entropy Algorithm with Image Segmentation. 2005
- [13] John C. Morrison, "Integrins in the optic nerve head: Potential roles in glaucomatous optic neuropathy (an American ophthalmological society thesis)".Trans Am Ophthalmol Soc/Vol 104/2006
- [14] Thomas M.Cover, and Joy A.Thomas, Elements of Information Theory. Second edition. Published by John Wiley & Sons, Inc.,Hoboken. 2006.

[15] D. Huang, E. A. Swanson, C. P. Lin, J. S. Schuman, W. G. Stinson, W. Chang, M. R. Hee, T. Flotte, K. Gregory, C. A. Puliafito, and J.G. Fujimoto, "Optical coherence tomography," *Science*, vol. 254, pp. 1178–1181, 1991.

[16] A. F. Fercher, C. K. Hitzenberger, W. Drexler, G. Kamp, and H.Sattmann, "In vivo optical coherence tomography," *Amer. J. Ophthalmol.*, vol. 116, pp. 113–114, 1993.

DISCLAIMER

The coding for this thesis was done using MATLAB 7.1 (version 7.1.0.246 August 02 2005).

APPENDIX

MATLAB Codes for digital image enhancement and information theory analysis.

1. Three Algorithms and Information Theory calculations

```
clear all
% 1. original image
M=imread('patientc07b.bmp');
figure(1),
subplot(2,2,1),
imshow(M)
title('(a) Original image');

% 2. wavelet image
im = double(M)/255;
hsv = rgb2hsv(im); %hsv image
V = hsv(:,:,3); %only operate in the v
[cA1,cH1,cV1,cD1] = dwt2(V,'haar');
cV1 = zeros(size(cV1));
cD1 = zeros(size(cD1));

f = fspecial('gaussian');

[cA2,cH2,cV2,cD2] = dwt2(cA1,'haar');
cA2 = imfilter(cA2,f,'replicate');
cV2 = zeros(size(cV2));
cD2 = zeros(size(cV2));

cA1 = idwt2(cA2,cH2,cV2,cD2,'haar',size(cA1));
cA1 = imfilter(cA1,f,'replicate');
newca = idwt2(cA1,cH1,cV1,cD1,'haar',size(V));
hsv(:,:,3) = newca;
rgb = hsv2rgb(hsv);
N1=rgb;
subplot(2,2,2),
imshow(N1,[]),title('(b) Wavelet image ');

% 3. Sobel image
% Sobel Method

I=M;
```

```

if ~(isa(I,'double') || isa(I,'single'));
I = im2single(I);
end

gh3= imfilter(I,fspecial('sobel')*2,'replicate');
filt = [.11 .11 .11; .11 .11 .11; .11 .11 .11];
n = 4;
In3 = gh;
for i = 1:n
    In3 =(bfilter(In3,filt));
    axis image
end
N2=In3;
subplot(2,2,3),
imshow(N2,[]);
title('(c) Sobel image');

% 4. YUV image
rgb=M;
ycbcr = rgb2ycbcr(rgb);
Y=ycbcr(:, :,1);
y1=imadjust(Y,[0.1 0.9],[],1.8);
ycbcr(:, :,1)=y1;
rgb2=ycbcr2rgb(ycbcr);
N3=rgb2;
%figure(4),
subplot(2,2,4),
imshow(N3)
title('(d) Contrast Adjustment image');

% (1) size of the image
[row col]=size(M)
entropy(M)
entropy(N1)
entropy(N2)
entropy(N3)
% entropy of each line in each image
for i=1:row
    a(i)=entropy(M(i,:));
    b(i)=entropy(N1(i,:));
    c(i)=entropy(N2(i,:));
    d(i)=entropy(N3(i,:));
end
max(a)

```

```

min(a)
max(b)
min(b)
max(c)
min(c)
max(d)
min(d)

if (ndims(M) == 3)
    M_1 = rgb2gray(M);
end
if (ndims(N1) == 3)
    N1_1 = rgb2gray(N1);
end
if (ndims(N2) == 3)
    N2_1 = rgb2gray(N2);
end
if (ndims(N3) == 3)
    N3_1 = rgb2gray(N3);
end
N1_1=abs(floor(N1_1*255));
N2_1=abs(floor(N2_1*255));

p1=imhist(M_1);
p2=imhist(N1_1);
p3=imhist(N2_1);
p4=imhist(N3_1);
t=0:1:255;
figure,
plot(t,p1,'g',t,p2,'b',t,p3,'-r',t,p4,'k')
axis([0 255 0 1000])
p1=imhist(M_1);p1 = p1/sum(p1);P1=p1(M_1+1);
p2=imhist(N1_1);p2 = p2/sum(p2);P2=p2(N1_1+1);
p3=imhist(N2_1);p3 = p3/sum(p3);P3=p3(N2_1+1);
p4=imhist(N3_1);p4 = p4/sum(p4);P4=p4(N3_1+1);

% relative entropy of each image and comparison
%relative entropy based on matrix of probability
for s=1:row
    for t=1:col/3
        if (P1(s,t)&P2(s,t)&P3(s,t)&P4(s,t))
            relative12(s,t)=P1(s,t)*log2(P1(s,t)/P2(s,t));
            relative13(s,t)=P1(s,t)*log2(P1(s,t)/P3(s,t));
            relative14(s,t)=P1(s,t)*log2(P1(s,t)/P4(s,t));
            relative21(s,t)=P2(s,t)*log2(P2(s,t)/P1(s,t));

```

```

relative31(s,t)=P3(s,t)*log2(P3(s,t)/P1(s,t));
relative41(s,t)=P4(s,t)*log2(P4(s,t)/P1(s,t));
end
end
end

```

```

RE12=sum(sum(relative12));
RE12
RE13=sum(sum(relative13));
RE13
RE14=sum(sum(relative14));
RE14
RE21=sum(sum(relative21));
RE21
RE31=sum(sum(relative31));
RE31
RE41=sum(sum(relative41));
RE41

```

```

p1=imhist(M_1);p1 = p1/sum(p1);P1=p1(M_1+1);
p2=imhist(N1_1);p2 = p2/sum(p2);P2=p2(N1_1+1);
p3=imhist(N2_1);p3 = p3/sum(p3);P3=p3(N2_1+1);
p4=imhist(N3_1);p4 = p4/sum(p4);P4=p4(N3_1+1);

```

```

for f=1:256
    if(p1(f)&p2(f)&p3(f)&p4(f))
        rela12(f)=p1(f)*log2(p1(f)/p2(f));
        rela13(f)=p1(f)*log2(p1(f)/p3(f));
        rela14(f)=p1(f)*log2(p1(f)/p4(f));
        rela21(f)=p2(f)*log2(p2(f)/p1(f));
        rela31(f)=p3(f)*log2(p3(f)/p1(f));
        rela41(f)=p4(f)*log2(p4(f)/p1(f));
    end
end

```

```

re12=sum(rela12)
re13=sum(rela13)
re14=sum(rela14)
re21=sum(rela21)
re31=sum(rela31)
re41=sum(rela41)

```

```

for f=1:256
    if(p1(f)&p2(f))

```

```

    r12(f)=p1(f)*log2(p1(f)/p2(f));
    r21(f)=p2(f)*log2(p2(f)/p1(f));
    end
end
for f=1:256
    if(p1(f)&p3(f))
        r13(f)=p1(f)*log2(p1(f)/p3(f));
        r31(f)=p3(f)*log2(p3(f)/p1(f));
        end
    end
for f=1:256
    if(p1(f)&p4(f))
        r14(f)=p1(f)*log2(p1(f)/p4(f));
        r41(f)=p4(f)*log2(p4(f)/p1(f));
        end
    end

    R12=sum(r12)
    R13=sum(r13)
    R14=sum(r14)
    R21=sum(r21)
    R31=sum(r31)
    R41=sum(r41)

%mutual information (maximum area)
p1=imhist(M_1);
p2=imhist(N1_1);
p3=imhist(N2_1);
p4=imhist(N3_1);
tolerance = 0.01;
p1 = 1-p1/sum(p1);
p2 = 1-p2/sum(p2);
p3 = 1-p3/sum(p3);
p4 = 1-p4/sum(p4);
P1 = p1(M_1+1);
P2 = p2(N1_1+1);
P3 = p3(N2_1+1);
P4 = p4(N3_1+1);
C12 = abs(P1 - P2) < tolerance;
Area12 = sum(sum(C12))% corresponds to the mutual information
C13 = abs(P1 - P3) < tolerance;
Area13 = sum(sum(C13))% corresponds to the mutual information
C14 = abs(P1 - P4) < tolerance;
Area14 = sum(sum(C14))% corresponds to the mutual information

```

2. Blurring Filter

```
function BlurF = bfilter(I, filt)
BlurF = zeros(size(I));
for i = 1:size(I,3)

    G = double(I(:, :, i));
    Gz = zeros(size(G)+2);
    Gz(1,:) = [G(1,1) G(1,:) G(1,end)]; % top
    Gz(end,:) = [G(end,1) G(end,:) G(end,end)]; % bottom
    Gz(2:end-1,1) = G(:,1); % left
    Gz(2:end-1,end) = G(:,end); % right
    Gz(2:end-1,2:end-1) = G; % overall
    Gf = conv2(Gz, filt); % Applying the filter
    BlurF(:, :, i) = Gf(3:end-2,3:end-2); % Removing the edges

end

% The for loop: fills up the top bottom and edges of the image
```

3. Comparison of sequential images using information theory

In order to avoid repeating the codes, we only list the important codes below. We have sequential images M and Ma. We use the codes above to obtain the Wavelet result, Sobel result and contrast adjustment result M1,N1,N2 and N3, respectively. For Ma, we have N1a, N2a and N3a.

```
size(M)
[rowa cola]=size(Ma)
if (ndims(M) == 3)
    M_1 = rgb2gray(M);
end
if (ndims(N1) == 3)
    N1_1 = rgb2gray(N1);
end
if (ndims(N2) == 3)
    N2_1 = rgb2gray(N2);
end
if (ndims(N3) == 3)
    N3_1 = rgb2gray(N3);
end
```



```

if (ndims(Ma) == 3)
    M_1a = rgb2gray(Ma);
end
if (ndims(N1a) == 3)
    N1_1a = rgb2gray(N1a);
end
if (ndims(N2a) == 3)
    N2_1a = rgb2gray(N2a);
end
if (ndims(N3a) == 3)
    N3_1a = rgb2gray(N3a);
end

N1_1=abs(floor(N1_1*255));
N2_1=abs(floor(N2_1*255));
N1_1a=abs(floor(N1_1a*255));
N2_1a=abs(floor(N2_1a*255));

p1=imhist(M_1);p1 = p1/sum(p1);P1=p1(M_1+1);
p2=imhist(N1_1);p2 = p2/sum(p2);P2=p2(N1_1+1);
p3=imhist(N2_1);p3 = p3/sum(p3);P3=p3(N2_1+1);
p4=imhist(N3_1);p4 = p4/sum(p4);P4=p4(N3_1+1);

p1a=imhist(M_1a);p1a = p1a/sum(p1a);P1a=p1a(M_1a+1);
p2a=imhist(N1_1a);p2a = p2a/sum(p2a);P2a=p2a(N1_1a+1);
p3a=imhist(N2_1a);p3a = p3a/sum(p3a);P3a=p3a(N2_1a+1);
p4a=imhist(N3_1a);p4a = p4a/sum(p4a);P4a=p4a(N3_1a+1);

for s=1:row
    for t=1:cola/3
        if (P1(s,t)&P2(s,t)&P3(s,t)&P4(s,t)&P1a(s,t)&P2a(s,t)&P3a(s,t)&P4a(s,t))
            relative0507a(s,t)=P1(s,t)*log2(P1(s,t)/P1a(s,t));
            relative0507b(s,t)=P2(s,t)*log2(P2(s,t)/P2a(s,t));
            relative0507c(s,t)=P3(s,t)*log2(P3(s,t)/P3a(s,t));
            relative0507d(s,t)=P4(s,t)*log2(P4(s,t)/P4a(s,t));
            relative0705a(s,t)=P1a(s,t)*log2(P1a(s,t)/P1(s,t));
            relative0705b(s,t)=P2a(s,t)*log2(P2a(s,t)/P2(s,t));
            relative0705c(s,t)=P3a(s,t)*log2(P3a(s,t)/P3(s,t));
            relative0705d(s,t)=P4a(s,t)*log2(P4a(s,t)/P4(s,t));
        end
    end
end

RE0507a=sum(sum(relative0507a));

```

```

RE0507a
RE0507b=sum(sum(relative0507b));
RE0507b
RE0507c=sum(sum(relative0507c));
RE0507c
RE0507d=sum(sum(relative0507d));
RE0507d

```

```

RE0705a=sum(sum(relative0705a));
RE0705a
RE0705b=sum(sum(relative0705b));
RE0705b
RE0705c=sum(sum(relative0705c));
RE0705c
RE0705d=sum(sum(relative0705d));
RE0705d

```

```

for s=1:row
    for t=1:cola/3
        %if (P1(s,t)&P2(s,t)&P3(s,t)&P4(s,t)&P1a(s,t)&P2a(s,t)&P3a(s,t)&P4a(s,t))
        relative0507a(s,t)=P1(s,t)*log2(P1(s,t)/P1a(s,t));
        relative0507b(s,t)=P2(s,t)*log2(P2(s,t)/P2a(s,t));
        relative0507c(s,t)=P3(s,t)*log2(P3(s,t)/P3a(s,t));
        relative0507d(s,t)=P4(s,t)*log2(P4(s,t)/P4a(s,t));
        relative0705a(s,t)=P1a(s,t)*log2(P1a(s,t)/P1(s,t));
        relative0705b(s,t)=P2a(s,t)*log2(P2a(s,t)/P2(s,t));
        relative0705c(s,t)=P3a(s,t)*log2(P3a(s,t)/P3(s,t));
        relative0705d(s,t)=P4a(s,t)*log2(P4a(s,t)/P4(s,t));
        end
    end
%end

```

```

REx0507a=sum(sum(relative0507a));
REx0507a
REx0507b=sum(sum(relative0507b));
REx0507b
REx0507c=sum(sum(relative0507c));
REx0507c
REx0507d=sum(sum(relative0507d));
REx0507d

```

```

REx0705a=sum(sum(relative0705a));
REx0705a
REx0705b=sum(sum(relative0705b));
REx0705b

```

```

REx0705c=sum(sum(relative0705c));
REx0705c
REx0705d=sum(sum(relative0705d));
REx0705d

p1=imhist(M_1);
p2=imhist(N1_1);
p3=imhist(N2_1);
p4=imhist(N3_1);
p1a=imhist(M_1a);
p2a=imhist(N1_1a);
p3a=imhist(N2_1a);
p4a=imhist(N3_1a);

for f=1:256
    %if(p1(f)&p2(f)&p3(f)&p4(f)&p1a(f)&p2a(f)&p3a(f)&p4a(f))
    re11a(f)=p1(f)*log2(p1(f)/p1a(f));
    re1a1(f)=p1a(f)*log2(p1a(f)/p1(f));
    re22a(f)=p2(f)*log2(p2(f)/p2a(f));
    re2a2(f)=p2a(f)*log2(p2a(f)/p2(f));
    re33a(f)=p3(f)*log2(p3(f)/p3a(f));
    re3a3(f)=p3a(f)*log2(p3a(f)/p3(f));
    re44a(f)=p4(f)*log2(p4(f)/p4a(f));
    re4a4(f)=p4a(f)*log2(p4a(f)/p4(f));
    end
%end
re1=sum(re11a)
re2=sum(re1a1)
re3=sum(re22a)
re4=sum(re2a2)
re5=sum(re33a)
re6=sum(re3a3)
re7=sum(re44a)
re8=sum(re4a4)

for f=1:256
    if(p1(f)&p1a(f))
        r11a(f)=p1(f)*log2(p1(f)/p1a(f));
        r1a1(f)=p1a(f)*log2(p1a(f)/p1(f));
    end
end
for f=1:256
    if(p2(f)&p2a(f))
        r22a(f)=p2(f)*log2(p2(f)/p2a(f));
        r2a2(f)=p2a(f)*log2(p2a(f)/p2(f));
    end
end

```

```

    end
end
for f=1:256
    if(p3(f)&p3a(f))
        r33a(f)=p3(f)*log2(p3(f)/p3a(f));
        r3a3(f)=p3a(f)*log2(p3a(f)/p3(f));
    end
end
for f=1:256
    if(p4(f)&p4a(f))
        r44a(f)=p4(f)*log2(p4(f)/p4a(f));
        r4a4(f)=p4a(f)*log2(p4a(f)/p4(f));
    end
end

```

```

R11a=sum(r11a);
R11a
R1a1=sum(r1a1);
R1a1
R22a=sum(r22a);
R22a
R2a2=sum(r2a2);
R2a2
R33a=sum(r33a);
R33a
R3a3=sum(r3a3);
R3a3
R44a=sum(r44a);
R44a
R4a4=sum(r4a4);
R4a4

```

%(5) mutual information (maximum area)

```

p1=imhist(M_1);
p2=imhist(N1_1);
p3=imhist(N2_1);
p4=imhist(N3_1);
p1a=imhist(M_1a);
p2a=imhist(N1_1a);
p3a=imhist(N2_1a);
p4a=imhist(N3_1a);

```

```

tolerance = 0.05;
p1 = 1-p1/sum(p1);
p2 = 1-p2/sum(p2);

```

```

p3 = 1-p3/sum(p3);
p4 = 1-p4/sum(p4);
P1 = p1(M_1+1);
P2 = p2(N1_1+1);
P3 = p3(N2_1+1);
P4 = p4(N3_1+1);

p1a = 1-p1a/sum(p1a);
p2a = 1-p2a/sum(p2a);
p3a = 1-p3a/sum(p3a);
p4a = 1-p4a/sum(p4a);
P1a = p1a(M_1a+1);
P2a = p2a(N1_1a+1);
P3a = p3a(N2_1a+1);
P4a = p4a(N3_1a+1);

Ccoma = abs(P1a - P1) < tolerance;
Areacoma = sum(sum(Ccoma))% corresponds to the mutual information
Ccomb = abs(P2a - P2) < tolerance;
Areacomb = sum(sum(Ccomb))% corresponds to the mutual information
Ccomc = abs(P3a - P3) < tolerance;
Areacomc = sum(sum(Ccomc))% corresponds to the mutual information
Ccomd = abs(P4a - P4) < tolerance;
Areacomd = sum(sum(Ccomd))% corresponds to the mutual information

%mutual information with position transformation (maximum area)

Areacoma=zeros(size(1,rowa));
Areacomb=zeros(size(1,rowa));
Areacomc=zeros(size(1,rowa));
Areacomd=zeros(size(1,rowa));

for xx=1:rowa
for tt=2:rowa
    m=P1a(1,:);
    P1a(tt-1,:)=P1a(tt,:);
    if (tt==(rowa))
        P1a(tt,:)=m;
    end
end
    Ccoma = abs(P1a - P1) < tolerance;
    Areacoma(xx) = sum(sum(Ccoma)); % corresponds to the mutual information
end
max(Areacoma)

```

```

for xx=1:rowa
for tt=2:rowa
    m=P2a(1,:);
    P2a(tt-1,:)=P2a(tt,:);
    if (tt==(rowa))
        P2a(tt,:)=m;
    end
end
Ccomb = abs(P2a - P2) < tolerance;
Areacomb(xx) = sum(sum(Ccomb)); % corresponds to the mutual information
end
max(Areacomb)

```

```

for xx=1:rowa
for tt=2:rowa
    m=P3a(1,:);
    P3a(tt-1,:)=P3a(tt,:);
    if (tt==(rowa))
        P3a(tt,:)=m;
    end
end
Ccomc = abs(P3a - P3) < tolerance;
Areacomc(xx) = sum(sum(Ccomc)); % corresponds to the mutual information
end
max(Areacomc)

```

```

for xx=1:rowa
for tt=2:rowa
    m=P4a(1,:);
    P4a(tt-1,:)=P4a(tt,:);
    if (tt==(rowa))
        P4a(tt,:)=m;
    end
end
Ccomd = abs(P4a - P4) < tolerance;
Areacomd(xx) = sum(sum(Ccomd)); % corresponds to the mutual information
end
max(Areacomd)

```

4. Correlation of the original images and results of three algorithms and intensity histograms

The same steps as above. We obtain M, N1.N2 and N3.

```

% find the histograms of the images(sections)
if (ndims(M) == 3)

```

```

    M_1 = rgb2gray(M);
end
if (ndims(N1) == 3)
    N1_1 = rgb2gray(N1);
end
if (ndims(N2) == 3)
    N2_1 = rgb2gray(N2);
end
if (ndims(N3) == 3)
    N3_1 = rgb2gray(N3);
end
a=imhist(M_1);
b=imhist(N1_1);
c=imhist(N2_1);
d=imhist(N3_1);

corrcoef(a,b)
corrcoef(a,c)
corrcoef(a,d)
corrcoef(b,c)
corrcoef(b,d)
corrcoef(c,d)

t=0:1:255;
figure,
%plot(t,a,'-g',t,b,':b',t,c,'--r')
plot(t,a,'-g',t,b,':b',t,c,'--r',t,d,'k')
%axis([200 255 0 80000])
xlabel('Intensity (From blackness to whiteness)')
ylabel('Frequency')
h = legend('Original image','Wavelet image','Sobel image','Contrast Adjustment image',4);
set(h,'Interpreter','none')
title('Histograms of Processed Images of Patient A in 06/14/2005')
%title('Histograms of Processed Images of Patient A in 06/12/2007')
%title('Histograms of Processed Images of Patient A in 05/29/2008')

%title('Histograms of Processed Images of Patient B in 03/09/2005')
%title('Histograms of Processed Images of Patient B in 04/11/2007')
%title('Histograms of Processed Images of Patient B in 04/18/2007')

```

5. Correlation of the sequential images and intensity histograms

```

clear all
%M=imread('patientb05.bmp');
%N1=imread('patientb07.bmp');
%N2=imread('patientb08.bmp');

```

```

M=imread('patientc05.bmp');
N1=imread('patientc07a.bmp');
N2=imread('patientc07b.bmp');

if (ndims(M) == 3)
    M_1 = rgb2gray(M);
end
a=imhist(M_1);

if (ndims(N1) == 3)
    N1_1 = rgb2gray(N1);
end
b=imhist(N1_1);

if (ndims(N2) == 3)
    N2_1 = rgb2gray(N2);
end
c=imhist(N2_1);

a=imhist(M_1);
b=imhist(N1_1);
c=imhist(N2_1);
corrcoef(a,b)
corrcoef(a,c)
corrcoef(b,c)

t=0:1:255;
figure,
plot(t,a,'-g',t,b,':b',t,c,'--r')
%axis([0 40 0 6000])
%title('Histograms of OCT Images of Patient A in Different Periods')
title('Histograms of OCT Images of Patient B in Different Periods')
xlabel('Intensity (From blackness to whiteness)')
ylabel('Frequency')
%h = legend('06/14/2005','06/12/2007','05/29/2008',3);
h = legend('03/09/2005','04/11/2007','04/18/2007',3);

set(h,'Interpreter','none')

```